5-2009

Finite Element Modeling of Full Depth Precast Concrete Transverse Bridge Deck Connections

Jacob Logan Julander
Utah State University

FINITE ELEMENT MODELING OF FULL DEPTH PRECAST CONCRETE TRANSVERSE BRIDGE DECK CONNECTIONS

by

J. Logan Julander

A thesis submitted in partial fulfillment
of the requirements for the degree

of

MASTER OF SCIENCE

in

Civil and Environmental Engineering

Approved:

_____	_____
Dr. Marvin Halling Major Professor	Dr. Paul Barr Committee Member
_____	_____
Dr. Joseph Caliendo Committee Member	Dr. Byron Burnham Dean of Graduate Studies

UTAH STATE UNIVERSITY
Logan, Utah

2009

ABSTRACT

Finite Element Modeling of Full Depth Precast Concrete

Transverse Bridge Deck Connections

by

J. Logan Julander, Master of Science

Utah State University, 2009

Major Professor: Dr. Marvin Halling
Department: Civil and Environmental Engineering

The frequent use of precast concrete panels has been used to decrease the construction time for bridges. Cracking often occurs at the transverse connections of these panels, resulting in corrosion, and decreased bridge life. Previous laboratory testing of these connections was performed at Utah State University for the Utah Department of Transportation to determine maximum shear and moment capacities, cracking behavior, and cracking loads for five different connections. Two connections are Utah Department of Transportation standard connections. These connections are post tensioned and welded tie connection using shear studs. A different type of welded tie connection using rebar was also tested, along with two prototype connections using a curved bolt to apply post tensioning. As part of this research finite element models were created using ANSYS software to confirm the tested results, and provide models for future analysis.

Moment-deflection and shear force-deflection curves were created using the results from the laboratory testing, and were compared with the results from the finite element analysis. The finite element models produced similar behavior and cracking loads when compared to the laboratory results. The curved bolt connections were found to be a good way of applying post tensioning.

(86 pages)

ACKNOWLEDGMENTS

First, I would like to thank my wonderful wife, Kaitlin, for all her help and support. I would like to thank the Utah Department of Transportation for funding this project. I would also like to thank Scott Porter for all of his assistance in the building and testing of the specimens.

The members of my graduate committee, Dr. Marvin Halling, Dr. Paul Barr, and Dr. Joseph Caliendo, have been a great support and fountain of knowledge for this project, and I would like to thank them.

Lastly, I want to thank Ken Jewkes and Wes Davidson for not only letting me use their laboratories and equipment, but also for teaching me to weld, use a torch, apply strain gages, and many other useful skills.

Logan Julander

CONTENTS

LIST OF TABLES

LIST OF FIGURES

LIST OF SYMBOLS

f'_c	Compressive strength of concrete
psi	Pounds per square inch
lb	Pounds
ksi	Kips per square inch
E	Modulus of elasticity of steel
ν	Poisson's ratio
f_y	Yield strength
E_t	Tangential modulus
θ	Rebar orientation angle in the XY plane
φ	Rebar orientation angle in the YZ plane
E_c	Modulus of elasticity of concrete
f_t	Uniaxial tensile cracking stress
f_{cb}	Biaxial compressive stress
σ_h	Ambient hydrostatic stress state
f_1	Biaxial crushing stress under the ambient hydrostatic stress state
f_2	Uniaxial crushing stress under the hydrostatic stress state
β_t	Shear transfer coefficient for open cracks
β_c	Shear transfer coefficient for closed cracks
v^1_r	Stiffness multiplier for cracked tensile condition
σ_{max}	Maximum normal contact stress
u^c_n	Contact gap at the completion of bonding

τ_{max}	Maximum tangential stress
u^c_t	Tangential slip at the completion of bonding
η	Artificial damping coefficient
β	Option indicator for tangential slip under compressive normal contact stress
K	Temperature in Kelvin
lb-ft	Pound feet
FKN	Normal penalty stiffness factor

CHAPTER I

INTRODUCTION

The Utah Department of Transportation (UDOT) has implemented the use of Accelerated Bridge Construction (ABC). This enables faster placement of concrete bridge decks and shortens bridge construction time. In ABC, a bridge deck is cast in manageable sections. These sections are transported to the bridge site and assembled. The bridge sections are connected to each other by grouted pockets. These connections do not behave as well as a cast in place deck, and often result in cracking at these grouted areas. When the concrete in these connections cracks it leads to the corrosion of the steel in the deck and the supporting members due to the infiltration of water and de-icing chemicals. Corrosion of the structural members could decrease the life of a bridge significantly. Cracking also weakens the joint which could lead to failure of the connection.

With the increased use of ABC, UDOT has developed new standard specifications, and has funded the testing of several of their connections, along with a new type of connection. This paper gives a brief overview of the results from the connection testing, but mainly focuses on the finite element modeling of the tested connections. For an in depth report on the laboratory testing of these connections refer to "Laboratory Testing of Precast Bridge Deck Panel Transverse Connections for Use in Accelerated Bridge Construction" by Scott Porter (Porter, 2009).

A finite element model was created using ANSYS (ANSYS, 2007) for each of the connections tested in the laboratory. The results from the model were compared to the tested results to better understand the cracking behavior of the connections. The purpose of this research was to create a preliminary finite element model that when compared and

matched with the tested results gives more information on the cracking behavior of each connection. This also allows for further analysis without the need of constructed specimens.

CHAPTER II

LITERATURE REVIEW

Finite element modeling is important in the study of precast concrete deck connections as it aids in evaluating results obtained from laboratory testing. If cracking can be represented in finite element analysis it would aid and simplify the studies of precast concrete bridge connections. An accurate working finite element model also allows for a larger range of analysis without the need of constructing physical specimens.

Different finite element models have been developed to confirm results from tested material. One common program for testing precast concrete bridges is ANSYS because of its built-in concrete capabilities and ability to perform nonlinear analysis. This aids in finding the initial cracking loads, and the location of these cracks.

Research done by Kachlakev, Miller, Yim (2001) on fiber reinforced polymer (FRP) retrofitted beams compared tested results to both linear and nonlinear finite element models. Two finite element programs that were used were SAP2000 (Computers and Structures, 1998) and ANSYS. The result shows that even in the linear range of the test ANSYS was closer to the test data than was SAP2000. This study tested both a control specimen and an existing bridge retrofitted with FRP laminates. The control specimen was tested to verify the efficacy of the finite element analysis. Then the bridge was modeled and compared with the test results from the existing bridge. The results indicated that the finite element model was stiffer than the existing bridge because of minor differences in material strengths and boundary conditions.

In a study performed by Bakhoum (1991), shear behavior between male-to-female connections were tested and compared with a finite element model. Several connections were modeled using ADINA (ADINA, 1986) finite element software which is able to model nonlinearity in different materials and the interface between them. This study is very helpful toward the process of finite element modeling. Both linear and nonlinear analysis were performed for the connection. The analysis included a model of the central part of the shear specimen, and a model of the entire shear specimen. It was determined that the entire specimen should be modeled when performing the shear analysis in order to obtain accurate results. The boundary conditions must also be well defined, or the results may be skewed. The model using linear analysis was approximately two times stiffer than the tested specimen. The nonlinear model increased the accuracy, but the first nonlinear model created did not give an accurate failure load. This was not obtained until accurate material parameters were entered, and proper strain softening and shear transfer coefficients were considered. The recorded deflections were applied to the model instead of applying loads. This was done to produce more accurate linear results. In this study Bakhoum stated that material failure envelopes are used to "establish uniaxial stress strain laws accounting for multiaxial stress conditions", and to indicate whether cracking or crushing has occurred.

Research by Issa et al. (1995a,b; Issa, Yousif, and Issa 1995; 2003) was performed on grouted female-to-female shear keyway connections. Issa tested different shapes of shear keyways, and found that the connection with 1-1/4" gap at the top and 1/2" gap at the bottom had the least amount of cracking in the connection. It was also suggested that post tensioning be applied to allow for proper sealing between the

connections. A finite element model was developed in ANSYS using SOLID65 elements which are able to model cracking and crushing of the grout. The analysis of the female-to-female shear keyway showed the major stress concentrations located in the grouting material along the connection joint and not in the concrete material. The model experienced cracking at the lower neck, and crushing at the upper neck of the model, with minor cracks in the concrete. The stress distributions across the connections were similar to the tested stresses, but the ultimate stress which occurred in the narrow neck of the connection had much higher stresses.

Sullivan (2007) analyzed transverse connections linearly in the finite element program SAP2000, and obtained nodal displacements and rotations. These values were then applied to the finite element model in ANSYS. This method of loading was similar to the method used by Bakhoum (1991). The loads were applied this way so that the analysis would be controlled by displacement rather than by an applied force which allowed for better convergence in the model. This study also used SOLID65 elements to model the concrete, but in places of irregular geometry SOLID45 elements were used. These elements were at the location of the connection, and did not have cracking capabilities.

CHAPTER III

LABORATORY TESTING

Connection Details

Each connection has a basic type of female-to-female shear keyway, with a different method of connecting the two panels together. Five different connection types were tested: 1) post tensioned, 2) 36 inch curved bolt, 3) 24 inch curved bolt, 4) welded rebar, and 5) welded stud.

Three of these connections, the post tensioned, 36 inch curved bolt, and 24 inch curved bolt connection, have an applied post tensioning to ensure strength across the grouted keyway. A connection commonly used by DOTs is the post tensioned connection. In practice post tensioning is applied by feeding either a rod, or cable longitudinally through the entire panel, and after the shear keyway is grouted the rods are tightened to apply a force of 300 psi across the face of the connection. In this experiment a harness was placed on the ends of the specimen and threaded rods connecting each harness were tightened to apply the required force for the post tensioned connection. An experimental type of post tensioning was developed by bending a threaded rod, feeding the rod through a conduit, and after grouting the connection applying the required force by tightening a nut on either end of the threaded rod. Two different lengths and diameters were used for these curved bolt connection, a 24 inch length with a 1 inch diameter bolt, and a 36 inch length with a 7/8 inch diameter bolt. The connection detail for these two curved bolt sections is shown in Figure 1.

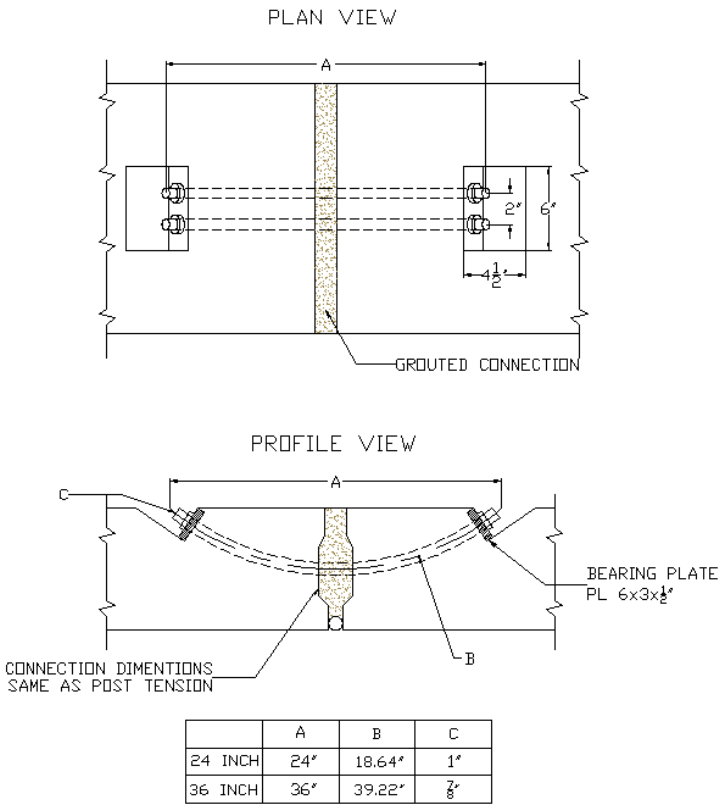

	A	B	C
24 INCH	24"	18.64"	1"
36 INCH	36"	39.22"	7/8"

Figure 1. Curved bolt connection detail.

The other two connections tested were the welded rebar, and the welded stud connections. These connections consist of a 6 inch wide plate cast into each side of a shear key with a rod welded between them. The plate was tied into the concrete panel by either a nelson stud or rebar welded to the plate. In this paper the connections will be referred to as welded rebar (Figure 2 a,b,c) and welded stud (Figure 2 d). In the welded rebar connection, the rebar extends into the concrete and ties into the panel reinforcement. The welded stud connection has two nelson studs that provide resistance against pullout of the plates. Both welded tie connections are nominally spaced at a maximum of every two feet. Between each of these welded tie portions is an unreinforced female-to-female shear key. The unreinforced section is shown in Figure 2(e).

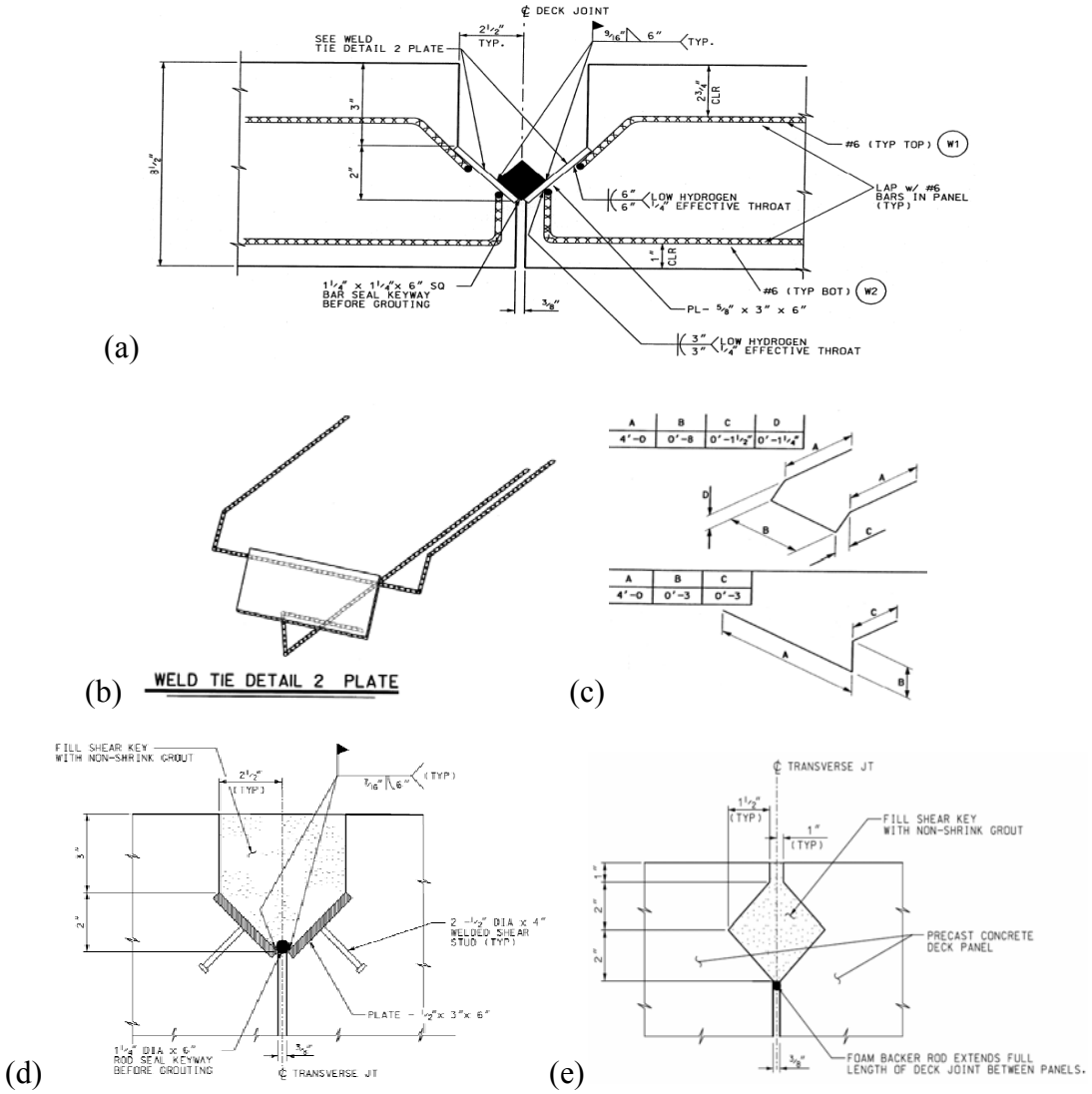

(a) Welded rebar (b) Rebar and plate detail (c) Rebar length detail (d) Welded stud (e) Unreinforced section (Utah Department Of Transportation 2008a)

Figure 2. Welded tie connection detail.

The post tensioned, and welded stud connections are UDOT ABC standard connections. The welded rebar connection was recently used on a bridge in Weber County, Utah (UDOT 2007), and Figure 2(a,b,c) were taken from those plans (UDOT 2008a,b,c). The two curved bolt connections were proposed by Hugh Boyle, an engineer and consultant on this project (personal communication Hugh Boyle).

Shear Specimen Details

The shear specimens consist of a 6 inch wide section of the connection with a depth of 8.75 inches. The layout for the shear specimens are shown in Figure 3, and have a similar design to the vertical shear tests performed in previous studies (Issa et al., 2003; Bakhourn, 1991; Biswas, 1986). However, in these studies there have been problems with failure occurring outside of the connection due to rotation of the upper and lower flanges. In order to avoid failure outside of the connection it was suggested that reinforcing rebar be used to reinforce the weaker areas. In this study #3 rebar sections were used to reinforce the flange. Another difference between this vertical shear specimen design and those used in other research is the gap between the flanges and the connection area. This gap was added to better test the interaction between the connection and concrete. This moves the area between the flanges and the represented deck away from the connection allowing for a shear failure angle, and better representation of the bridge thickness. A deeper gap (approximately three inches) was used for the welded stud and rebar specimens to allow more room for welding in the connection.

The shear specimens were loaded monotonically to failure using a basic push off method. The load was applied by two hydraulic rams pulling down on a hollow square section of steel (Figure 3 b,c). A load cell was placed at the point of loading and a spherical head was used to maintain a constant downward force despite irregularities in the specimen or loading equipment. A harness restrained the specimen from rotation and separating at the connection as is shown in Figure 3. A linear variable displacement transducer (LVDT) was used to measure deflection, and a 50,000 lb capacity load cell

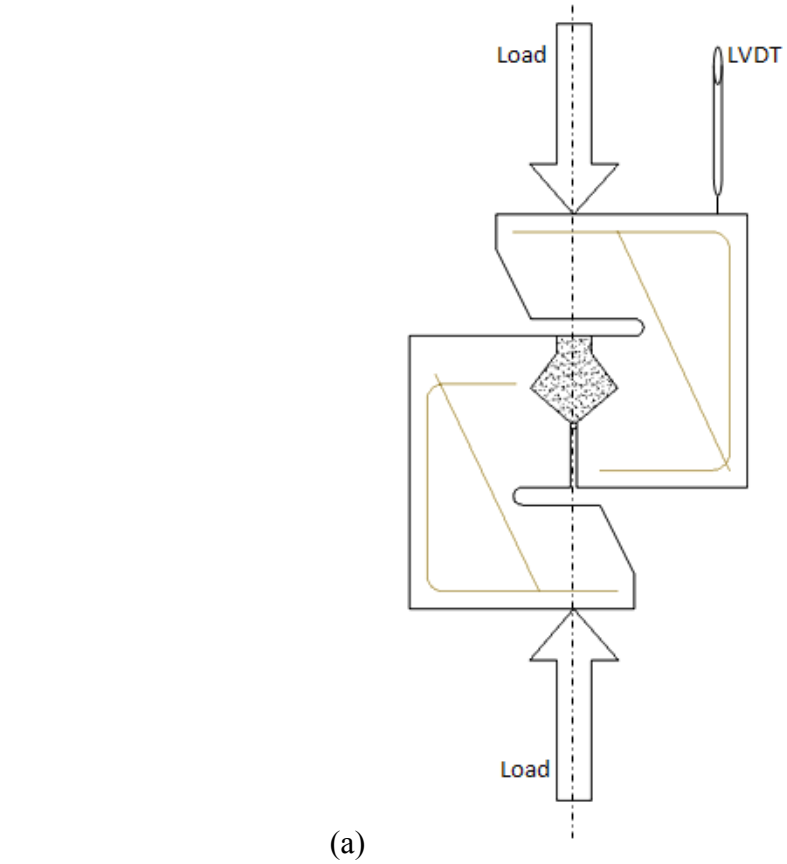

(a)

(b)

(c)

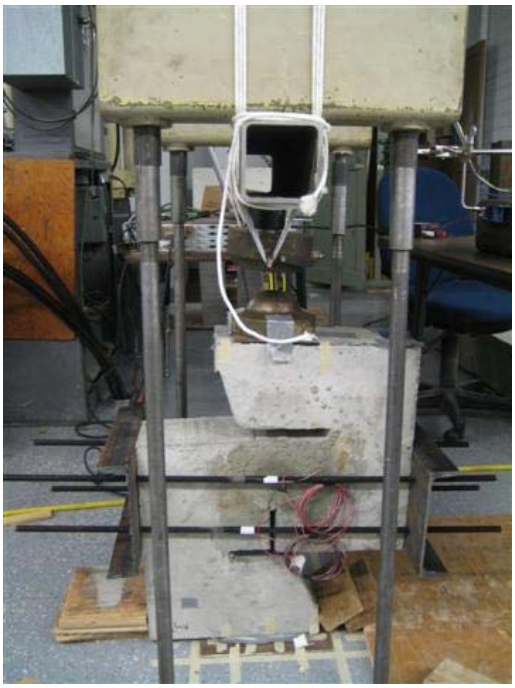

Figure 3. Shear specimen test setup (Porter, 2009).

was used to measure the applied force. The output from both LVDT and load cell were recorded using the Vishay data acquisition program Strain Smart. These results were used to obtain the maximum shear force, and to create a load verses deflection curve, from which a cracking load could be determined.

Shear Test Results

The connection types tested for shear were: 1) post tensioned, 2) post tensioned keyway without post tensioning, 3) welded stud, 4) welded rebar, and 5) the unreinforced section of the welded tie connection. The non-post tensioned connection was tested to calculate the shear force gained from applying post tensioning. The welded rebar specimens experienced failure in the upper and lower flanges away from the connection. Because their ultimate capacity was never obtained they are not included in the shear specimen results. As aforementioned the welded tie connections are comprised of both welded portion and unreinforced connection. Both were tested separately for shear and an average force per length is shown in the Table 1.

At least three specimens of each type of connection were tested for ultimate shear capacity and averaged per foot of connection. In Table 1 these values were normalized to

Table 1. Shear specimen ultimate capacities

Connection	Average Ultimate Shear Capacity (lb/ft)	Ultimate Shear Capacity/Capacity of Post Tensioned Connection
Post tensioned	49345	1.00
Non-Post Tensioned	12733	0.26
Welded Stud	42684	0.87
Welded Stud 6” spaced 18”	36055	0.73
Welded Stud 6” spaced 24”	21706	0.44
Unreinforced Portion of Welded Tie	14713	0.30

Table 2. Shear specimen cracking capacities

Connection	Average Cracking Shear Capacity (lb/ft)	Cracking Shear/Ultimate Shear Capacity
Post tensioned	42500	0.99
Non-post Tensioned	11000	0.85
Welded Stud	19600	0.42
Unreinforced Portion of Welded Tie	11800	0.40

the post tensioned connection because of its wide use in ABC. The post tensioned connection had the greatest shear strength. The ratio of the non-post tensioned connection to the post tensioned is 0.26, and shows the increase that post tensioning provides. The ratio of the unreinforced section to the post tensioned is 0.30, and when combined with the welded stud section increases the ratio to 0.44 and 0.73 for a 24 inch and 18 inch spacing respectively.

During testing a rough approximation of initial cracking was recorded with a corresponding load. A ratio was calculated of the cracking strength to ultimate capacity for each connection. The post tensioned had the highest cracking shear strength at 21,250 lb which is approximately 99% of its average ultimate shear strength. The non-post tensioned connections had the lowest cracking strength at 5,500 lb, or 85% of the average ultimate capacity for this connection. These two connections experienced failure immediately after cracking. The welded stud had the second highest cracking strength of 9,800 lbs that accounted for 42% of its average ultimate capacity. The unreinforced welded tie connection had a cracking strength of 5,900 which occurred at 40% of its average ultimate capacity.

Flexural Specimen Details

Each of the flexural specimens was 72 inches long, 18 inches wide, and 8.75 inches deep. This was considered an adequately represented section of the bridge deck. The two welded tie connections had the 6 inch connection in the center, and 6 inches of the unreinforced keyway on each side. The panels were reinforced with #6 rebar as specified in the UDOT ABC standards. Additional reinforcement was placed at the loading point to avoid shear failure away from the connection. These beam specimens were tested monotonically until failure using four point loading. The load was applied using hydraulic rams that pulled down on a wide flange beam, which transferred the load

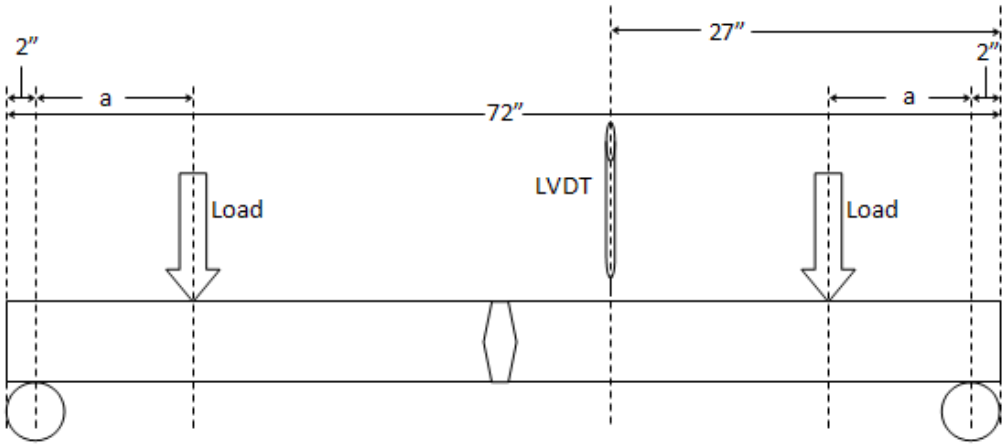

(a) (b)

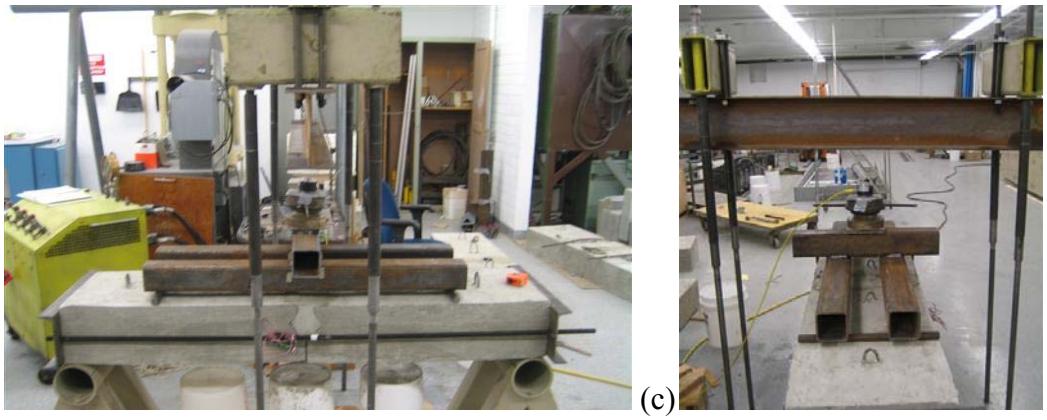

(c)

Figure 4. Flexural specimen test setup (Porter, 2009).

to a load spreader which applied the load at two different points on the specimen. During initial testing the load spreader's bearing points were 12 inches from each end, but due to excessive loads (close to 50,000 lb, the load cells capacity), the bearing points were moved to 24 inch from each end. This is illustrated in Figure 4. A 50,000 pound load cell was used to record the applied load, and an LVDT was placed at 27 inches from the right end of the beam and was used to record deflection.

Flexural Specimen Results

The connection types tested for moment capacity are: 1) welded stud, 2) welded rebar, 3) post tensioned, 4) 24 inch curved bolt, and 5) 36 inch curved bolt. As the post tensioned connection is a highly used connection in ABC, the other connections capacities were normalized to its moment capacity (17,261 lb-ft). The flexural results are shown in Table 3. As you can see from the table, the 36 inch curved bolt unexpectedly had the greatest capacity, and a ratio of 1.19 when compared to the post tensioned connection. The 24 inch curved bolt connection did not perform as well and had a ratio of 0.70 compared to the post tensioned connection. The welded rebar connection had a higher moment capacity than the post tensioned connection with a ratio of 1.05. The

Table 3. Flexural specimen ultimate capacities

Connection	Average Moment Capacity (lb-ft)	Capacity/Capacity of Post Tensioned Connection
Welded Stud	6667	0.39
Welded Rebar	18047	1.05
Post Tensioned	17261	1.00
24-inch Curved Bolt	12079	0.70
36-inch Curved Bolt	20623	1.19

welded stud had the least amount of moment capacity, failing at 0.39 times the post tensioned ultimate capacity.

Also during flexural testing, approximate cracking moments were recorded and averaged for each connection. Similar to the shear results the average cracking moment was compared to the ultimate moment capacity of the connection, and can be found in Table 4. The welded rebar, and post tensioned connections both had the highest average cracking moment at 10,400 lb and 10,300 lb respectively, which is approximately 60% of the ultimate capacity of the two connections. Although the 36 inch curved bolt had the highest moment capacity of the connections, its cracking moment was lower than the welded rebar and post tensioned connections (8,100 lb), accounting for 40% of its ultimate capacity. The 24 inch curved bolt and welded stud connections had the smallest cracking moment at 4,000 lb and 3,300 lb respectively. The 24 inch curved bolt connection cracked at approximately 48% of its ultimate moment capacity, and the welded stud cracked at 52% of its ultimate capacity.

Table 4. Flexural specimen cracking moment

Connection	Average Cracking Moment (lb-ft)	Cracking Moment/Ultimate Moment Capacity
Welded Stud	3300	0.52
Welded Rebar	10400	0.60
Post Tensioned	10300	0.61
24-inch Curved Bolt	4000	0.48
36-inch Curved Bolt	8100	0.40

CHAPTER IV

FINITE ELEMENT MODELING

Element and Material Properties

The finite element program ANSYS 11 was used to create and analyze models of all the tested connections. This software was chosen because of its capacity to model cracking in concrete. Models were developed for both shear and moment testing, and load deflection and moment deflection curves were plotted for comparison with the laboratory testing.

The material properties for the elements used in this analysis are defined by four different categories: element type, real constant, material model, and key options. The element types for the models are SOLID65, SOLID45, and LINK8. Real constants are inputs that describe the geometry for LINK8 elements and rebar specifications for SOLID65 element. Material models are the linear and nonlinear properties that define the elements' behavior. The material models used in this research were linear, bilinear isotropic hardening, and the built in material model for concrete. Key options (KEYOPT) inputs determine whether to include or disable certain element functions. Default KEYOPTs are used for all the elements except SOLID65 and contact elements. Each element will be described with its corresponding real constants and material models in the following paragraphs.

LINK8 elements are line elements with three translational degrees of freedom. These were used to model the steel plate, welded rebar, shear studs, and other rebar reinforcement within the panel. The real constant input for a LINK8 element is the cross

sectional area. Linear and nonlinear material models were used for the LINK8 element. The linear model properties are the modulus of elasticity (E) and Poisson's ratio (ν). These values for steel are E = 29,000,000 psi and ν = 0.2. Bilinear isotropic hardening was the model used to simulate yielding in the steel, and had a yielding stress (f_y) of 60,000 psi, and a tangential modulus of elasticity (E_t) of 2,900 psi. The modulus and yielding stress are in accordance with UDOT's specifications for structural steel for these connections.

SOLID45 components are eight node 3D elements with three translational degrees of freedom. In this research these elements act as bearing plates to reduce major stress concentrations in the models at the loading and bearing points. SOLID45 elements do not have a real constant, and has the same linear material properties as the LINK8 element (E = 29,000,000 psi, ν = 0.2). These plates are used for modeling purposes, and are not representative of physical plates used during laboratory testing.

SOLID65 elements are eight node 3D solid elements with three translational degrees of freedom at each node, and are used to model the concrete and grout. The real constant for a SOLID65 element indicate the material, volume ratio, and direction of reinforcement in the element. As opposed to using a line element to model rebar in discrete locations, a built in reinforcement option, known as smeared reinforcement was used. This method was implemented to simplify the modeling of reinforcement in the panel. The material for the smeared reinforcement is input by using the predefined material model number. The volume ratio is the ratio of the reinforcement volume over the total element volume (ANSYS, 2007). The direction of the reinforcement is indicated by two angles (θ and φ). The angle θ is measured from the X to the Y axis, and φ is the

angle to the Z axis. The real constant for the SOLID65 element has the option of reinforcement in three different directions, but in this analysis only the Y and Z direction were used. Reinforcement in the X direction was omitted to avoid having the reinforcement acting at the connection.

Both linear and nonlinear material models were used for SOLID65 elements. The linear properties include the modulus of elasticity (E_c) and Poisson's ratio (ν). The modulus of elasticity for concrete and grout was calculated using the following equation:

$$E_c = 57000\sqrt{f_c'}$$

where f'_c is the uniaxial compressive stress and values for the concrete and grout are 4,000 psi, and 6,000 psi, respectively. These values are the specified compressive strength for concrete used in ABC, and three day compressive strength indicated by the grout manufacturers. The Poisson's ratio for each was taken as 0.3.

The nonlinear material model used for SOLID65 elements was the concrete model which predicts the failure of brittle materials. A failure surface is defined by five different stress parameters: uniaxial tensile cracking stress (f_t), uniaxial compressive stress ($f_c^{'}$), biaxial compressive stress (f_{cb}), ambient hydrostatic stress state (σ_h), biaxial crushing stress under the ambient hydrostatic stress state (f_1), and uniaxial crushing stress under the hydrostatic stress state (f_2).

Concrete tensile tests were performed on cylinders made from the concrete used in the specimens, resulting in an average tensile strength of 480 psi. Because of convergence problems in ANSYS, the crushing feature was turned off using a value of -1.

This was done to save computational time and focus on the cracking that occurs within the specimens. Crushing has been turned off in other studies because it was problematic towards obtaining an accurate solution (Kachlakev, Miller, and Yim, 2001; Wolanski, 2004). By doing this, the material cracks whenever the principle stress component is higher than the tensile stress of the concrete and the remaining parameters (f_{cb}, f_1, and f_2) are suppressed (ANSYS, 2007).

Three other inputs for the concrete model are shear transfer coefficient for open cracks (β_t), shear transfer coefficient for closed cracks (β_c), and stiffness multiplier for cracked tensile condition (v^1_r). Shear transfer coefficients range from values of 0.0 to 1.0 with 0.0 representing a smooth crack with no shear transfer, and 1.0 representing a rough crack that transfers the entire shear. For this analysis β_t was set to 0.2 representing a fairly smooth crack, and β_c was set to 0.6 representing a moderately rough crack. A value of 0.2 was suggested in Wolanski (2004) because when β_t for an open crack drops below 0.2 convergence is difficult to achieve. The value of the stiffness multiplier for cracked tensile condition was taken as the default value v^1_r=0.6.

KEYOPTs are used in SOLID65 elements to help solution convergence. KEYOPTs are different for each element, and for the SOLID65 elements key option (7) is used to help convergence when the element is undergoing cracking. KEYOPT(7) was set to a value of 1 which gives the option to include tensile stress relaxation after cracking. When a crack occurs in an analysis the stress available at that node drops to zero, which often causes convergence problems. Stress relaxation allows for a more gradual reduction helping in obtaining a converged solution.

Initially the concrete to grout contact was modeled as continuous, but analysis showed that the concrete separating from the grout had a significant impact in the force deflection curve. In order to model the bond and separation of the concrete and grout contact pairs with debonding capabilities were implemented. Contact pairs consist of two elements: a target element (TARGE170) and a contact element (CONTA173). These elements define the boundary between the surfaces of the concrete and grout, and have the ability to model delamination of the two surfaces. The TARGE170 elements overlay a 3D solid element and characterize the boundary conditions. These are associated with the contact elements by sharing a real constant set. The CONTA173 element is able to model surface to surface contact between 3D solid elements. The stiffness between the surface and target can be modified to define the bond characteristics.

The real set constants for contact pairs have the option of 26 inputs, however, only one of these inputs were changed from the default settings. Initial analysis of each model without using contact pairs had a linear region before cracking that was far more rigid than the tested specimens. This suggests that there is some softening in this initial region. To imitate this initial softening, the normal penalty stiffness factor (FKN) was reduced.

CONTA173 elements have twelve key options available, and five were changed from their default values (2,5,9,10,12). KEYOPT(12) indicates the initial bond behavior of the contact pairs. In this analysis the bond is represented as fully bonded by setting KEYOPT(12) to 5, and the separation is modeled using a cohesive zone material model. KEYOPT(2) controls the contact algorithm, which was changed to the penalty method as suggested when KEYOPT(12) is changed to a value of 5. The penalty method is a contact

algorithm which defines the stiffness between the two surfaces as a spring whose stiffness is equal to the FKN value (ANSYS, 2007). The stiffness was updated after each iteration by changing KEYOPT(10) to a value of 2. While constructing the model an initial gap was found between the concrete and grout. This gap was insignificant, but potentially detrimental to the analysis. Using KEYOPT(9) and (5) equal to 1 the initial gap was neglected.

In order to allow for separation between the grout and the concrete a Cohesive Zone Material Model (CZM) was used. This works by a constitutive relationship between the traction on the interface, and the corresponding separation across the interface (ANSYS, 2007). The bond between the concrete and grout was defined by using the real constant for the contact pairs, and the CZM material model inputs.

The CZM model has bilinear behavior by using one of two set options; traction and maximum separation, or traction and release energy. In this analysis the traction and maximum separation was used which has 6 input option; maximum normal contact stress (σ_{max}), contact gap at the completion of bonding (u^c_n), maximum tangential stress (τ_{max}), tangential slip at the completion of bonding (u^c_t), artificial damping coefficient (η), and an option indicator for tangential slip under compressive normal contact stress (β). Because sliding does not control the separation only σ_{max} and u^c_n were used in the CZM. The artificial damping is included to compensate for convergence problems that are caused by modeling debonding. The damping input has units of time and is multiplied by the smallest time increment. ANSYS suggests the value be between .1 and .01; in this analysis the value was taken as the minimum suggested value of .01 for all the models.

A static analysis was performed for each of the models and a full Newton-Raphson method was used for the nonlinear analysis. The load was divided into multiple substeps until the final load was achieved. The load step increment was chosen by ANSYS, so if the solution was not converging at a certain load substep, the increment decreased until convergence was reached. The number of substeps was increased until a full analysis was reached for the load step. While developing different models, properties and meshes were changed, and some analyses would not converge. In order to exit an analysis that is not converging a maximum number of equilibrium equations was set. This number was set from 50 to 200 equations depending on the type of connection and model. The ANSYS code for each model is found in Appendix A.

Shear Finite Element Modeling

In order to obtain a consistent mesh with the differing geometry, the order and creation of the model and mesh were critical. The process is shown in Figure 5. The models were divided into a series of quadrilaterals with keypoints inserted at the corners of these areas as shown in Figure 5(a). From these keypoints a parallel plane of keypoints were generated, and solids were created between the two planes using the keypoints as shown in Figure 5(b,c). The individual solids were connected using the ANSYS Boolean Glue function, and adjacent lines and keyponts were combined into one. By doing this the individual solids are still able to maintain their different properties. All solids of one type were selected, and the corresponding properties were assigned before a volume was meshed.

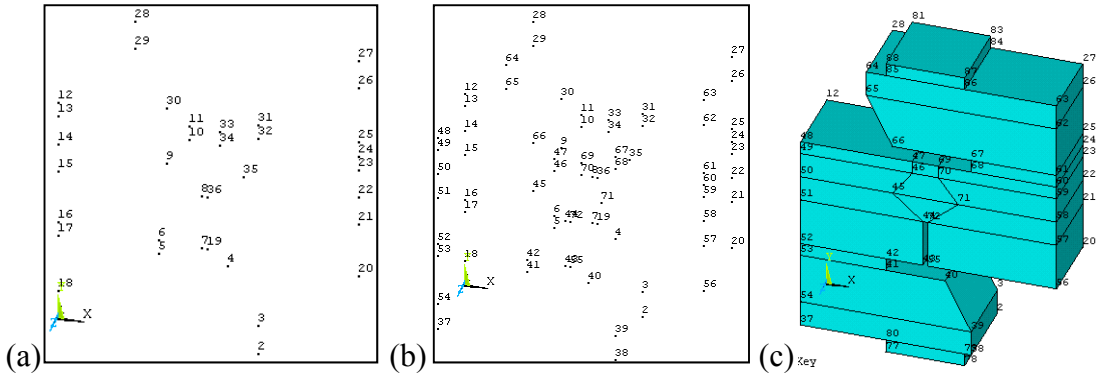

Figure 5. Shear model creation sequence.

To create line elements such as a shear stud, a line is selected from a volume, assigned the reinforcement properties, and meshed. Because of this process, the solids were divided in order to create boundaries where line elements could be assigned. The welded stud model has a plate on an angle with shear studs perpendicular to the plate. In order to create a boundary line where the stud was located, certain volumes were divided at angles creating geometry that is difficult to mesh. At these locations some triangular meshes were used. Triangular shapes are not recommended for use in SOLID65 elements, and are used only where no other option could be found.

The geometry for the shear models were the same as the geometry for the tested specimens. SOLID45 elements were used to model a 6” x 6” x 1” bearing plate located at the loading points, and centered over the connection. Figure 6 shows the steps in applying the boundary conditions. The bottom plate was fixed against translation in the Y direction (Figure 6 a), the right and left outside face of the model was fixed against translation in the X direction (Figure 6 b), and the back face of the model was fixed against translation in the Z direction (Figure 6 c). The load was applied to the top of the upper plate evenly distributed at the nodes (Figure 6 d).

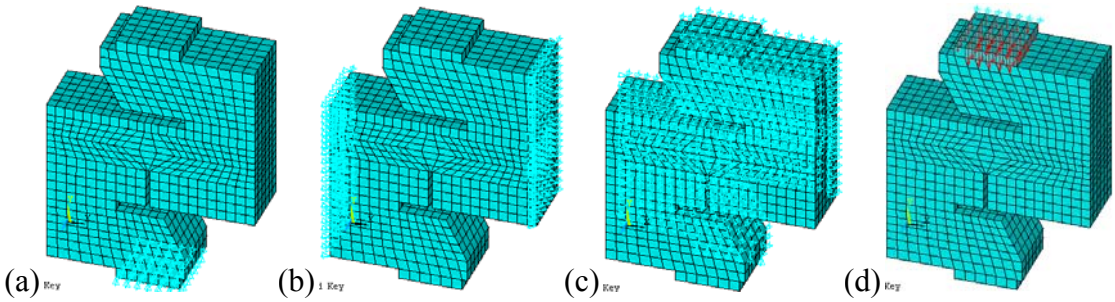

Figure 6. Shear model boundary conditions sequence.

The welded stud connection was created by using LINK8 elements for the steel plates and shear studs. The steel plate could not be modeled with a plate element because it has rotational degrees of freedom which would create inconsistencies along the boundary of the solid elements which have only translational degrees of freedom. The cross sectional area for the line elements used to model the plates was 1.277 in^2 and the area for the welded studs were 0.2 in^2.

UDOT requires that at least 300 psi be applied across the face of the connection for adequate post tensioning. In the post tensioned model, a horizontal pressure of 300 psi was applied to the outside left face of the model and an analysis was performed to ensure that 300 psi was acting across the face of the connection before the vertical load was applied.

Some properties in the models were changed in order to better model the behavior of the different connections. The concrete, grout, and steel properties were consistent for all the shear models. The properties changed were the variables affecting the contact behavior between the concrete and the grout which are, σ_{max}, u^c_n, and FKN. The value for σ_{max} is 480 psi, the same value as the tensile strength for the concrete. u^c_n was taken as

0.015 inches, representing a relatively small separation between the concrete and grout upon failure of the bond. The value for FKN that was used was 0.0011 for the shear specimens. This value is multiplied by the normal contact stiffness resulting in relatively low contact stiffness. During testing it was observed that the bond between the concrete and the grout was very weak, and separation often occurred along this boundary. Because of this weak bond the normal contact stiffness was reduced.

Flexural Finite Element Modeling

The flexural models were created similar to the shear models – keypoints were created, solids were generated from those keyponts, and assigning and meshing of the solids was performed. However, due to symmetry, one quarter of the geometry was modeled in ANSYS, and proper boundary conditions were applied at the plane of symmetry. The specimen was divided lengthwise along the centerline and then fixed against movement in the X direction on that face. Likewise, the model was divided widthwise, and fixed against translation in the Z direction along the face of the divide as is shown in Figure 7. A 9” x 4” x 1” solid with steel properties was modeled at the loading and bearing points – on top of the beam 22 inches from the left hand side and at the bottom left corner – to avoid stress concentrations. The beam was modeled as simply supported by pinning the nodes along the center of the bearing plate in the Y direction. This was suggested by Kachlakev, Miller, and Yim (2001) to allow for rotation and avoid cracking in the concrete around the bearing plate. The load was distributed to the nodes along the center of the loading plate. The loading plate was moved 12 inches from the

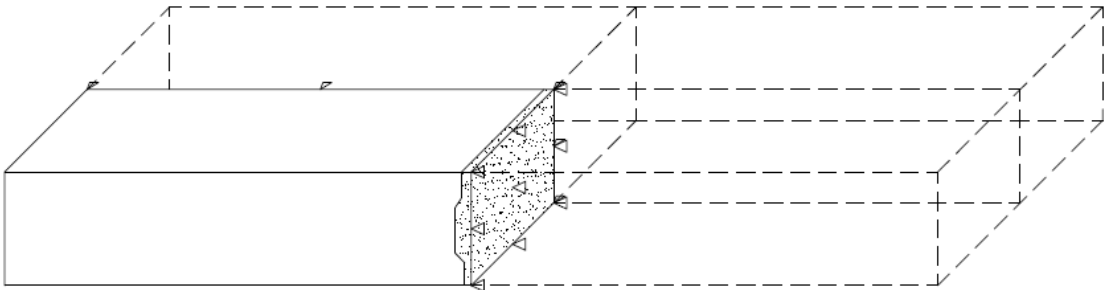

Figure 7. Quarter scale flexural model.

right side for the 24 inch curved bolt model because the 4 inch plate interfered with one end of the curved bolt. Because of the different geometry of each model, a uniform mesh could not be obtained, but a one inch element size was attempted for each model.

In order to model the post tensile force for the simple post tensioned models, a uniform pressure of 300 psi was applied over the area on the right end of the model. A test was run without applying a vertical force, and the stresses were analyzed to ensure that 300 psi was acting across the connection.

In the laboratory testing the curved bolt connection was made by bending threaded rods to a specific curvature and feeding that through oversized conduits across the connection. After the grout was placed steel plates with holes were placed on the ends of the rods and nuts were used to tighten the bolt to the post tensile force. This was modeled in ANSYS using LINK8 elements with steel properties for the curved bolts. The curved portion of the bolt was simplified as several linear elements, which were connected to the concrete and grout elements at specific nodes. The post tensioned force was modeled by applying a temperature differential across the curved bolt elements. A coefficient of thermal expansion of 12×10^{-6} in/K was used and temperatures were changed until an average stress of 300 psi was observed across the connection. In

addition the strain was output for the curved bolt and compared to the strain obtained through laboratory testing, and final minor temperature adjustments were made to match the tested strain. For the 24 and 36 inch curved bolt the temperature difference was -115 K, and -130 K, respectively.

The contact pairs behave differently when used in shear dominated analysis and bending dominated analysis. Some of the contact inputs have been changed for this reason. The value for σ_{max} remained the same value as the tensile strength of the concrete (480 psi). Except for the welded stud connection, the value of u^c_n was kept at 0.015 inches. In this connection the contact gap affected the results significantly whereas the other connection showed little change. The welded stud had the best results when u^c_n was set at 0.016 inches. The value for FKN was changed to from 0.0011 to 0.0036 for the flexural specimens. Also the cracking coefficients β_t, and β_c for the welded rebar connection were changed from 0.2 and 0.6 to 0.9 and 0.9, respectively. Since little separation occurred between the grout and concrete in this connection the resultant cracks were very rough.

CHAPTER V

RESULTS AND COMPARISON

Shear Finite Element Model Results

The applied load and deflection were recorded at each incremental loadstep. The nodal deflection was recorded in the center of the specimen one inch from the right edge on the top flange. This was the approximate location of the LVDT during the physical testing. Cracking sequences were also recorded for each connection. The four different models analyzed in shear are: 1) unreinforced portion of the welded tie, 2) welded stud, 3) non-post tensioned, and 4) post tensioned.

In ANSYS when the principle stress at an integration point in a concrete element exceeds the tensile stress, cracking occurs. This is modeled by an adjustment of the material properties and is called a "smeared crack" or region of cracking. Cracking is available in three orthogonal directions at each integration point which is indicated by a red (first crack), green (second crack), or blue (third crack) circle. The cracking represented from the finite element model is not a finite crack, but an area where cracking occurs. Cracking in multiple directions indicates considerable cracking, and is regarded as a location where visible cracking can occur. A more detailed description of the finite element predicted cracking sequence will be given for each connection.

Similar to the tested results, the finite element models also experience cracking in the flanges away from the connection. However, in the analysis, the arm did not fail, but continued to crack which did not result in cracking in the connection until very high loads (nearly double the ultimate load of the tested specimens). To better model the behavior of

the specimens two options were modified. First, the concrete crushing and cracking capabilities were turned off for all the concrete that was part of the upper and lower flanges to better localize cracking in the connection. Second, contact pairs were used at the interface between the concrete and the grouted connection. These changes produced a behavior in the model that was similar to the tested model.

The result from the unreinforced portion of the welded tie connection is used to illustrate the accuracy gained from using contact pairs. After each analysis a force deflection curve was created using the applied load and deflection from each substep. The deflection was measured at the approximate location where the deflection was recorded during the laboratory testing. Figure 8 shows the load-deflection curve for the tested specimens and two results from the ANSYS models. The finite element model without the contact pairs is approximately 21 times stiffer than the model with contact pairs. The force-deflection curve of the model with the contact pairs more accurately follows the approximate curve of the tested specimens.

The model behaved similarly to the tested connections with separation in the concrete and grout in the upper left and lower right portions of the keyway. After this initial separation the deflection continued linearly until the ultimate load. The connection also had cracking comparable to the tested specimens. Figure 9 shows the cracking sequence of the unreinforced welded tie specimen tested on December 10th. Figure 9(a) shows the separation of the concrete from the grout in the upper left and lower right portion of the shear key. Initial cracking starts at the upper right portion of the shear key and continues at approximately a 45° angle. This crack spreads into the grout at the same angle and fails along that plane. Figure 10 shows the cracking sequence that ANSYS

predicts. The first initial crack occurs also on the upper right hand side of the shear key. In Figure 10(b-d) cracking spreads from the right corner of the shear key, and downward into the deck area, but multiple cracks primarily occur in the upper right hand portion. In Figure 10(e,f) shows cracking through the grouted portion at approximately a 45° angle.

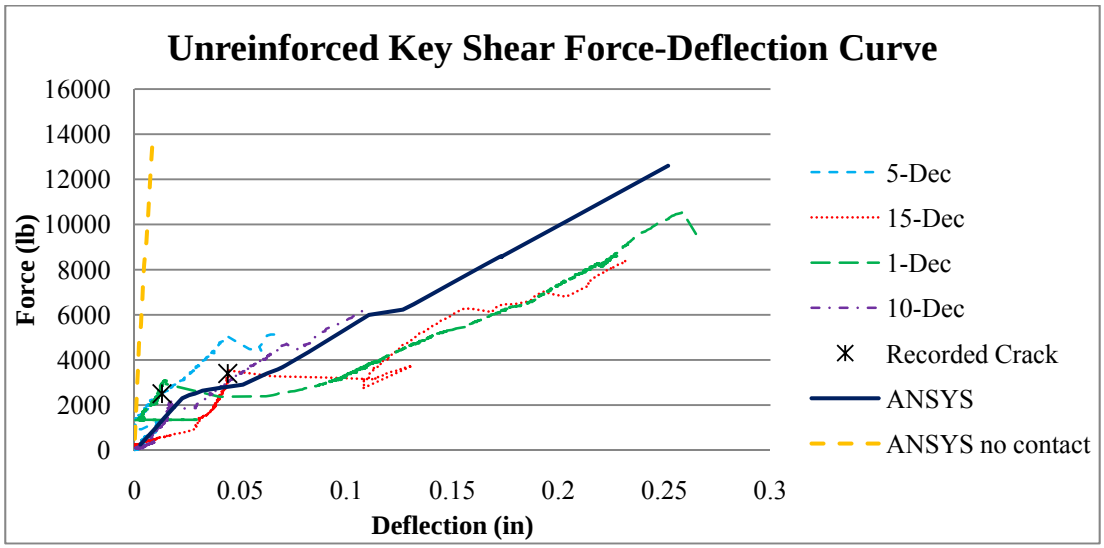

Figure 8. Unreinforced key shear force-deflection curves.

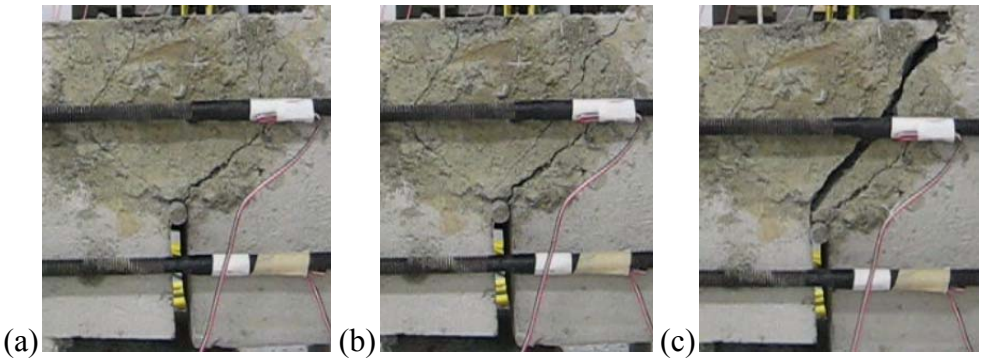

Figure 9. Shear unreinforced welded tie tested cracking sequence.

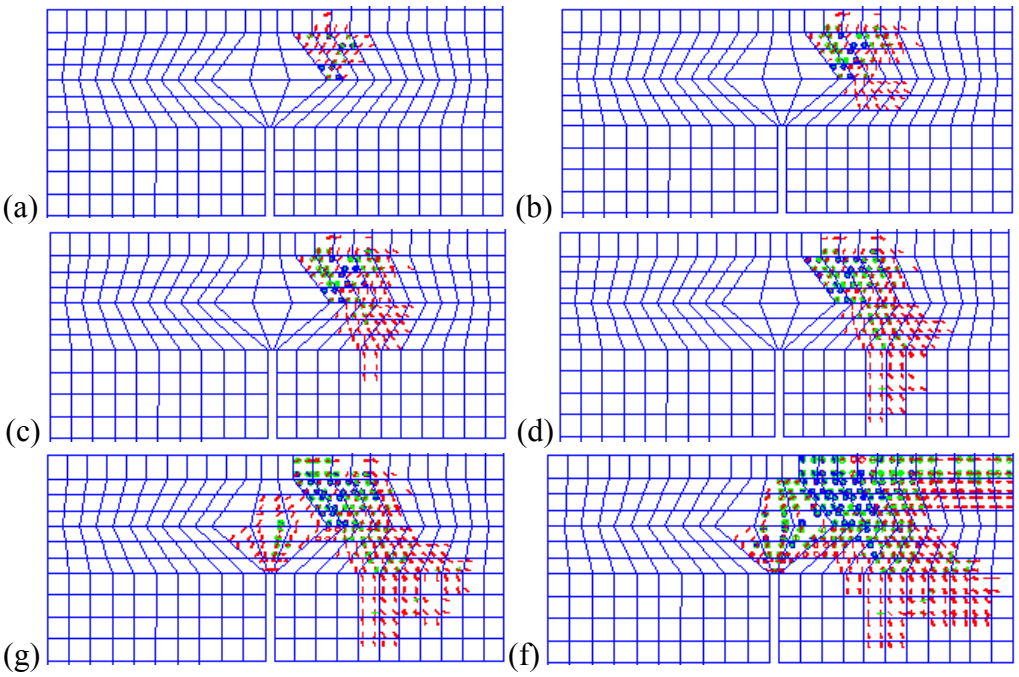

Figure 10. Shear unreinforced welded tie finite model cracking sequence.

The force deflection curves for the welded stud connections are shown in Figure 11. The finite model for the welded stud connection follows the tests results except for the December 5th test which has a greater deflection. The points where there are loops in the curves are when cracking occurs in the flange which caused rotation in the specimen. This caused the LVDT to rise and fall rapidly, and does not have a correct correlation with the deflection occurring in the connection. The finite element model follows the tested results approximately until this point. Once major cracking occurs the modeled connection has a linear deflection.

The cracking sequence for the welded stud specimen tested on December 10th is shown in Figure 12. In the figure, initial separation occurs between the concrete and grout in the upper right hand side of the pocket. Cracking starts at the location of the welded studs on the left side of the figure as seen in the second picture. This crack continues till

the bottom of the connection, and cracking through the bottom of the grouted portion can be seen. Another crack forms along on the opposite side along the welded stud. Towards failure cracking occurs through the grout at an angle of approximately 30°. Many of the

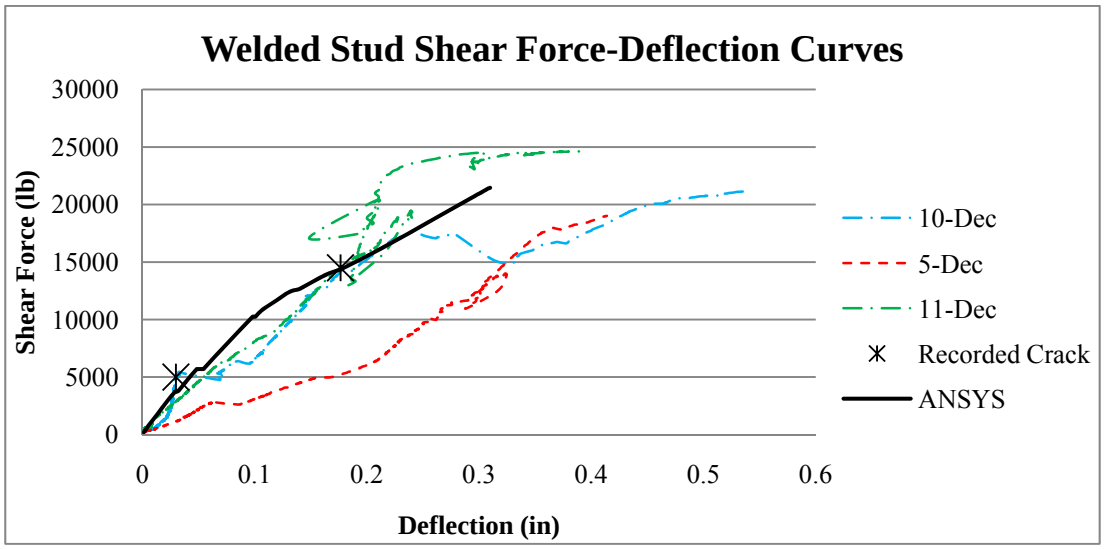

Figure 11. Welded stud shear force-deflection curves.

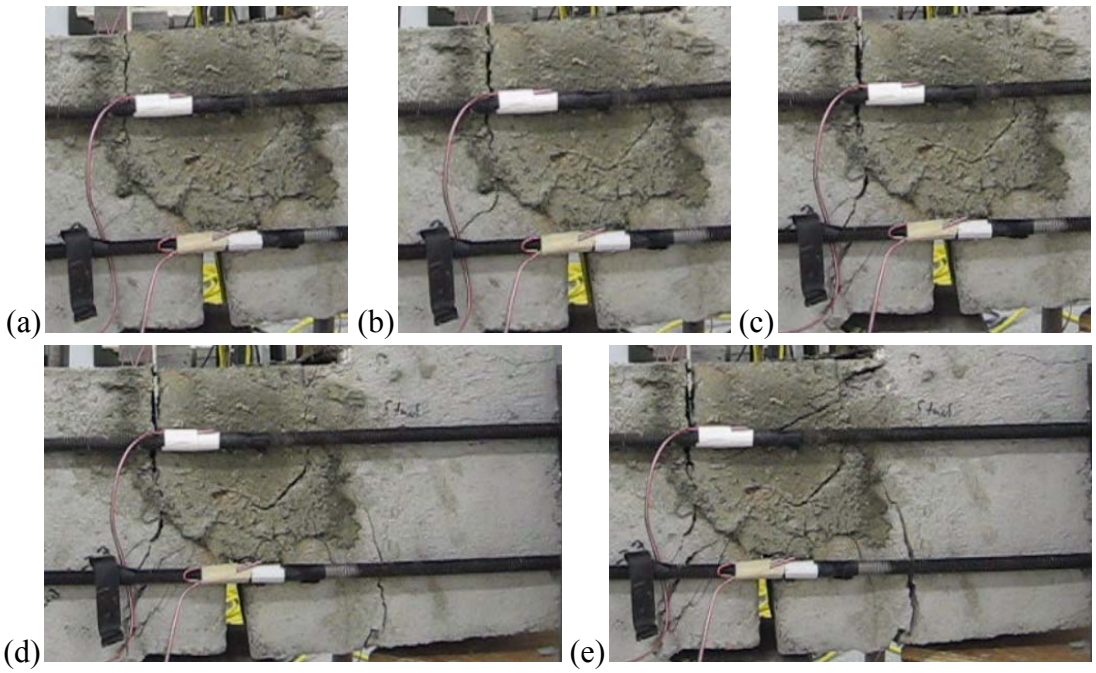

Figure 12. Shear welded stud tested cracking sequence.

specimens experienced cracking in the flanges away from the connection, the test from December 10th experiencing the least amount of cracking in the flanges.

Comparatively ANSYS predicts cracking similar to the tested sequence. Figure 13 show that cracking sequence begin at the point where the welded studs are located. This figure does not show the separation because it is not considered cracking, but it is to be noted that separation between the grout and concrete does occur in the finite model. Figure 13(b) shows the cracking in the grout at approximate a 30° angle. Figure 13(c-e) shows the cracking continuing down the path of the welded stud, and across the grouted pocket. Towards the end of the analysis major cracking occurs on the right side of the model, and upper left portion.

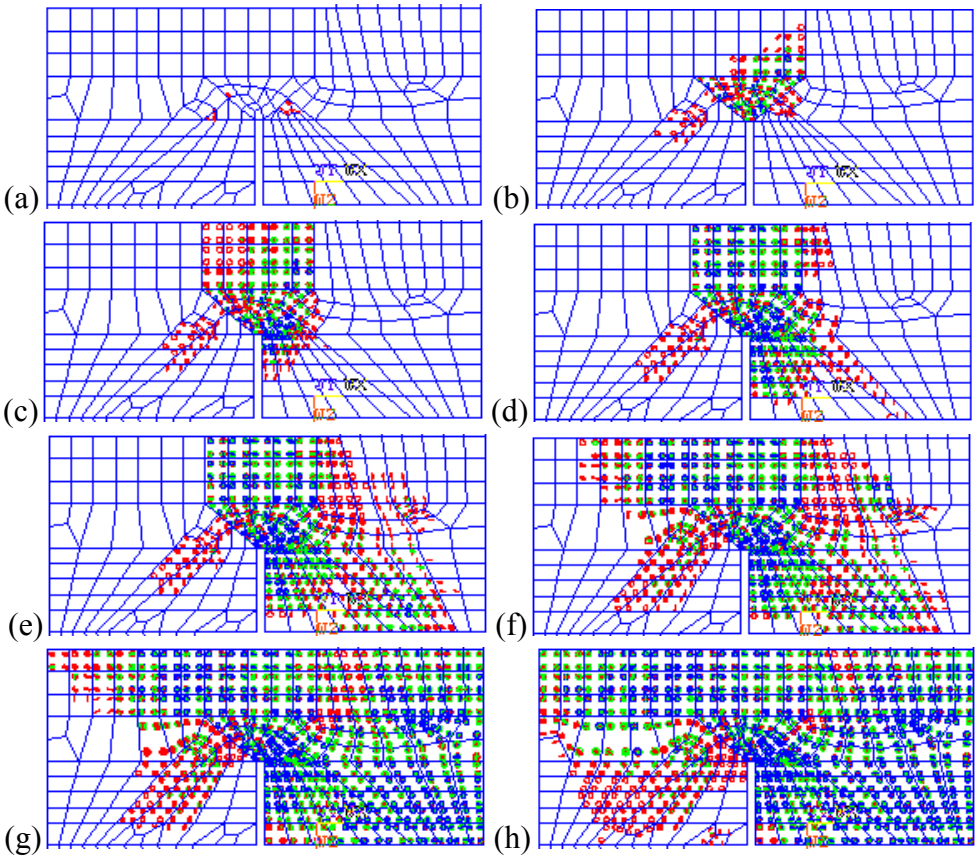

Figure 13. Shear welded stud modeled cracking sequence.

Only two specimens of the non-post tension connection were tested for shear. These were tested to find the strength gained in applying post tensioning to this specific female-to-female connection. The force-deflection curve for the non-post tensioned connection is fairly simple, and is shown in Figure 14. The finite element model follows the curve of the specimen tested on December 11th, but tends to be more rigid than the tested specimens. Cracking occurs in the model at the point on the graph where the curve flattens out (approximately 7,400 lb). This agrees with the tested specimens where failure occurs immediately after cracking.

The cracking sequence for the specimen tested on December 11th is shown in Figure 15. This is compared with Figure 16 which shows the finite element cracking sequence. These figures show cracking along the boundary of the grouted pocket, and a cracking at about a 60° angle.

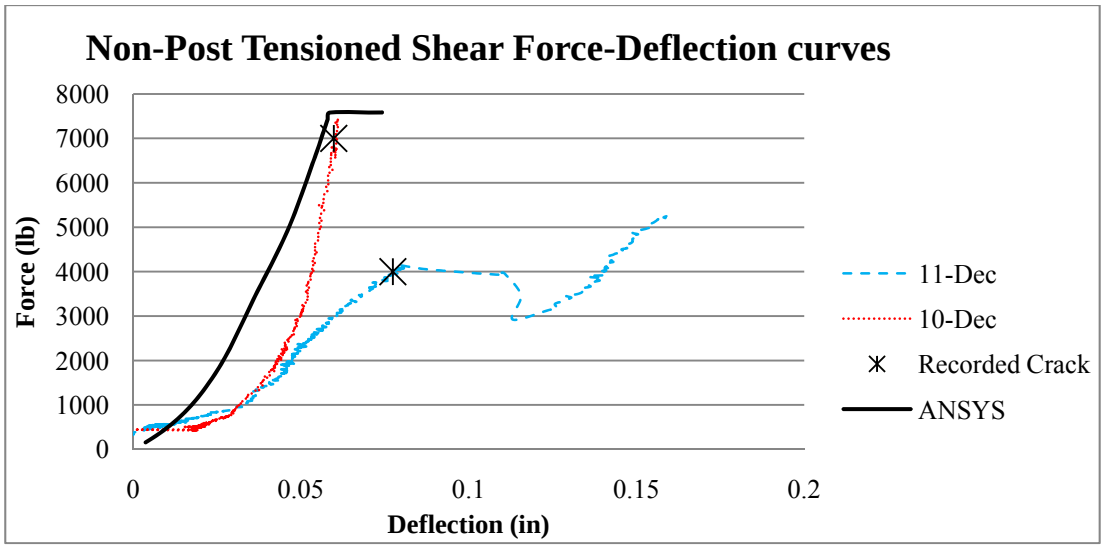

Figure 14. Non-post tensioned shear force-deflection curve.

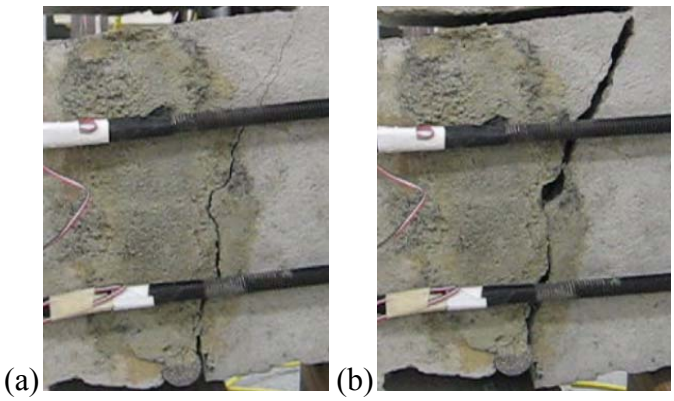

Figure 15. Shear non-post tensioned tested cracking sequence.

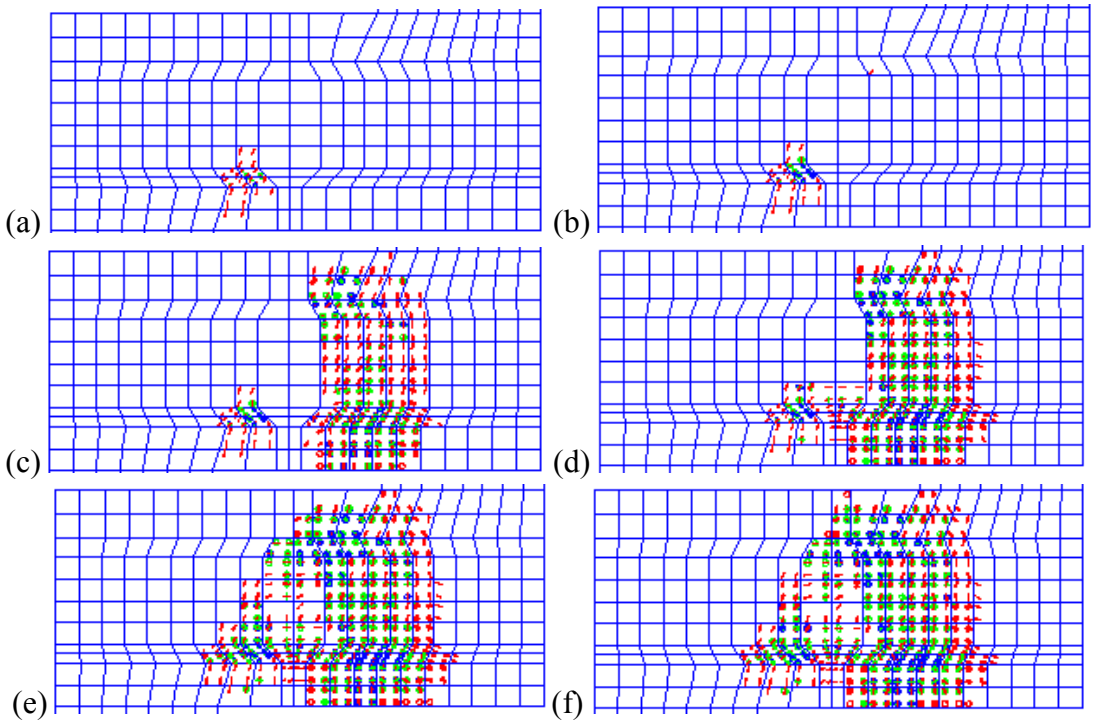

Figure 16. Shear non-post tensioned modeled cracking sequence.

The finite element analysis for the post tensioned connection closely follows the results from the specimen tested on December 11th, as shown in Figure 17. The model is slightly more rigid than the mentioned specimen results, but follows the same trend in curvature.

The initial cracking is lower than the observed cracking in all tested cases. The cracking sequence however has a similar pattern in the finite model and the tested results. The cracking sequence for a specimen tested on December 12th is shown in Figure 18. Like the non-post tensioned models, the post tensioned models fail shortly after cracking occurs. All of the tested models experienced cracking in the flanges. Figure 18 shows the first visible cracks occurring in the flanges, and the cracking in the connection occurring at the bottom left and top right corners of the connection. These cracks continue toward the connection at an angle between 30° and 45°, and continue along the boundary between the concrete and grout. The predicted cracking also begins in the flanges as is shown in Figure 19 (a). Cracking in the connection begins at the upper right hand side, and lower left hand side, and continue through the grouted pocket (Figure 19 b-d).

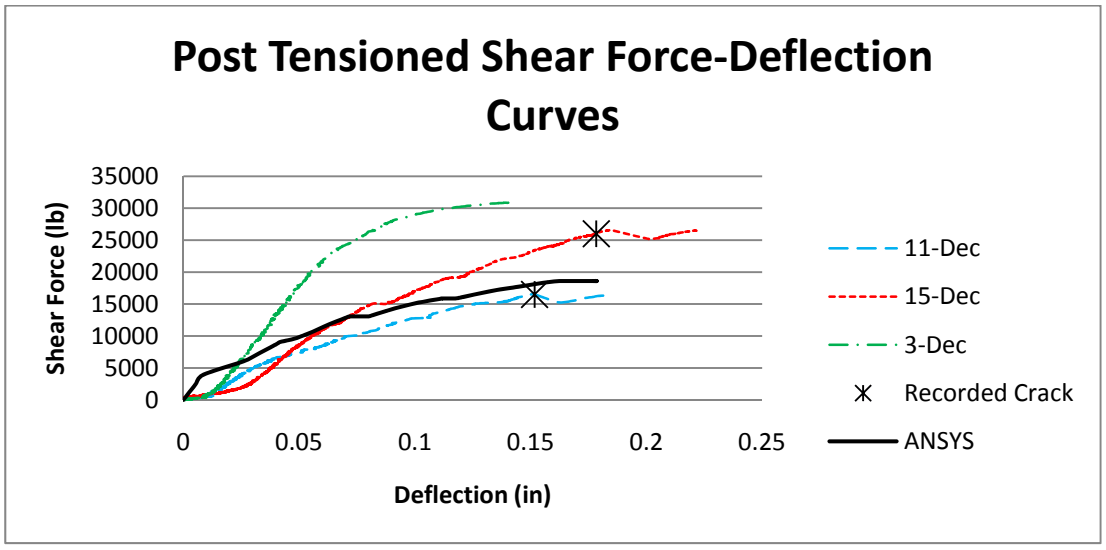

Figure 17. Post tensioned shear force-deflection curves.

(a) 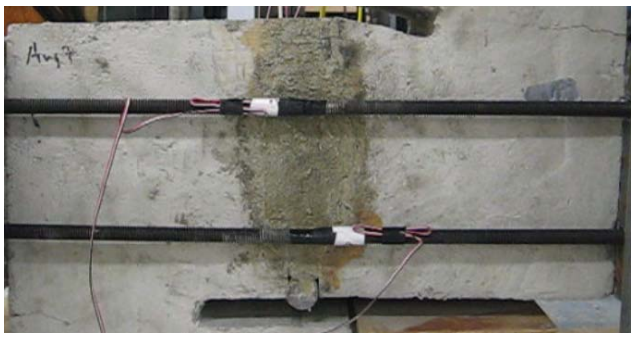 (b) 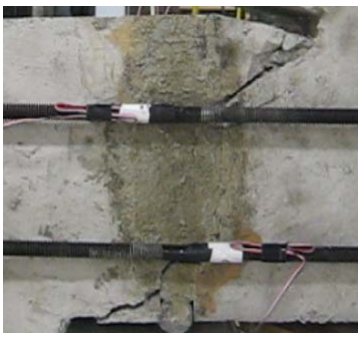

Figure 18. Shear post tensioned tested cracking sequence.

(a) 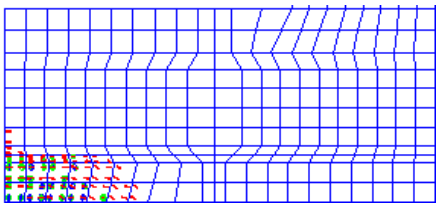 (b) 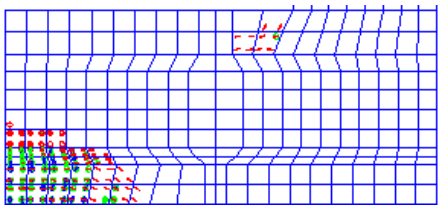

(c) 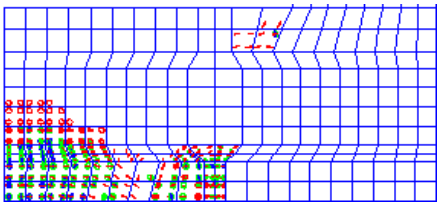 (d) 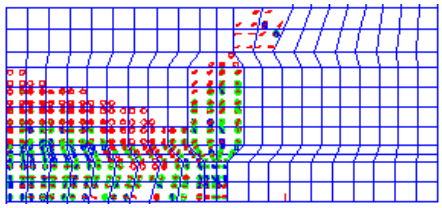

(e) 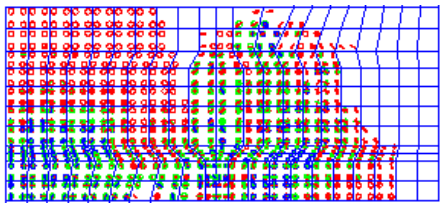

Figure 19. Shear post tensioned modeled cracking sequence.

Flexural Finite Element Model Results

The ultimate load capacities for the laboratory tests were applied to the finite element models and analyses were performed. The load was recorded at each substep, and nodal deflections were obtained at a location 27 inches from the left side of the beam, as was performed during laboratory testing. Moment-deflection curves were created for

each type of connection using these recorded deflections and loads. The five different connections that were modeled are: 1) post tensioned, 2) welded rebar, 3) welded stud, 4) 36 inch curved bolt, and 5) 24 inch curved bolt. Images of crack progression were captured for each of the models and compiled into figures. These figures show the grouted connection with approximately five inches on either side of the connection for the laboratory tested specimens. Because half of the specimen was modeled in the finite element analysis, the figures for the predicted cracking show only half of the specimen.

Similar to the shear models, contact pair elements were used to mimic the concrete to grout bond and add an initial softening that occurs in the tested specimens. Without the contact pairs the moment-deflection curve for the post tensioned connection resulted in an initial slope that was approximately 8 times larger than the tested results.

The moment-deflection curves for the post tensioned connection are found in Figure 20. The ANSYS curve follows the tested curves almost exactly in the linear range prior to cracking. After cracking the finite element model follows the results from the specimen tested on January 30th. The cracking moment for the finite element model is 13,982 lb-ft.

Figure 22 shows the cracking sequence calculated by ANSYS, and Figure 21 shows the cracking sequence for the laboratory tested specimen. In the tested specimen the cracking initiates in the top narrow neck of the connection as shown in Figure 21(a-c). This crack continues into the concrete, and in the final steps separation occurs at the bottom between the concrete and the grout. The cracking sequence as predicted in ANSYS shows the cracking initiating in the concrete at the bottom portion of the connection as shown in Figure 22(a). This cracking continues upward and along the

connection. Cracking in the grout occurs in the last two steps in the figure, and begins in the bottom of the grouted pocket and moves upwards.

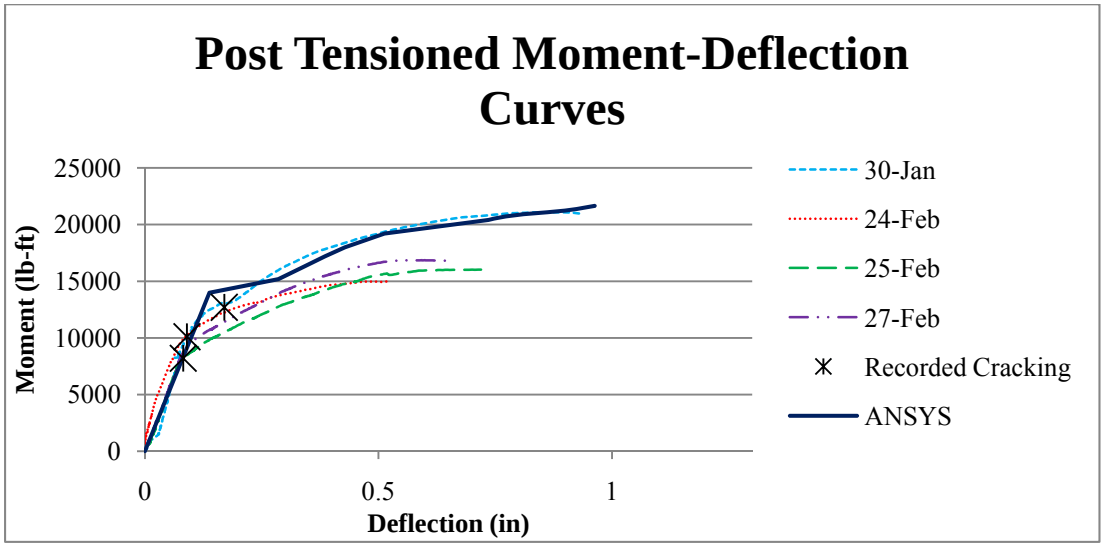

Figure 20. Post tensioned moment deflection curves.

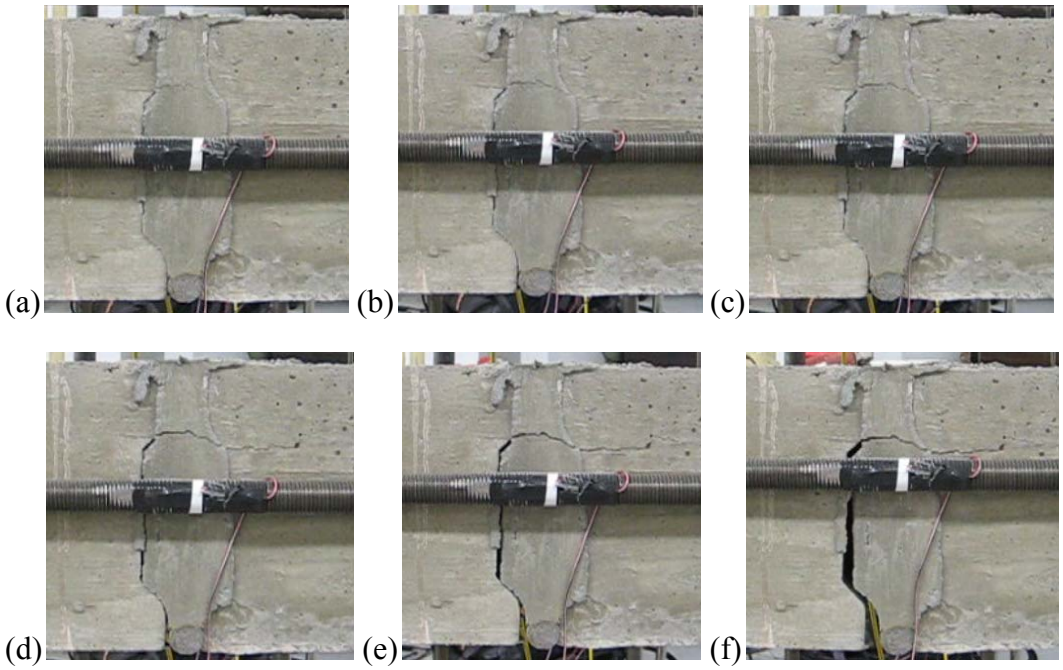

Figure 21. Flexural post tensioned tested cracking sequence.

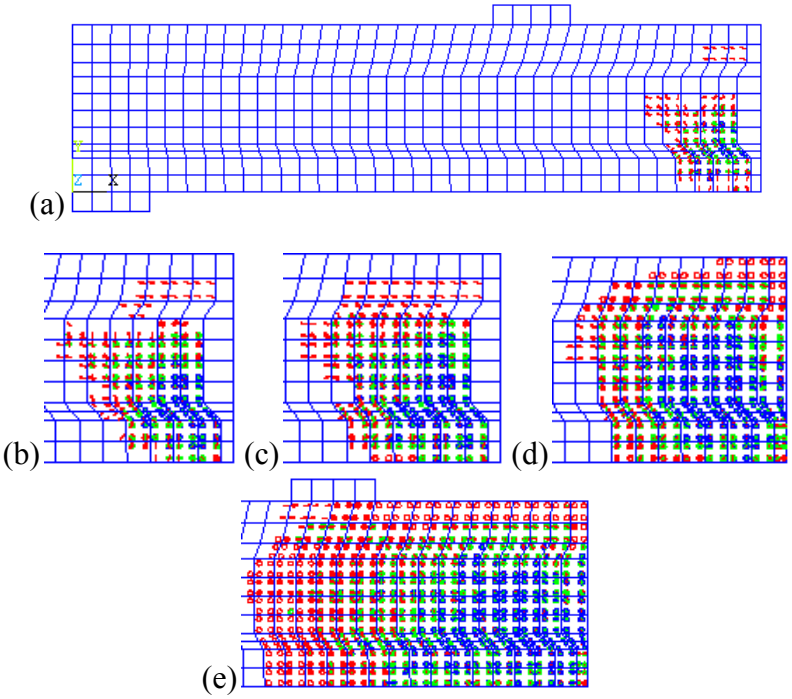

Figure 22. Flexural post tensioned modeled cracking sequence.

The moment-deflection curve for the welded stud model closely follows the tested results as is shown in Figure 23. The curve follows the connection tested on February 4th, which is the test with the highest concrete strength. The cracking moment that occurs in the model is at 1,764 lb-ft, which is relatively low compared to the observed cracking moment recorded from the tested specimens. However, there is a second point of cracking where major deflection occurs, and this point is considerably closer to the observed cracking moment. This happens at 3,284 lb-ft and is recognized as the first plateau seen on the moment-deflection graph.

The cracking sequence for the laboratory tested and computer modeled specimens can be seen in Figure 24 and Figure 25, respectively. Observed cracking initiates at the bottom of the concrete specimen approximately where the end of the welded stud lies.

Cracking continues along the width of the slab, and small cracks can be seen near the corner of the connection in Figure 24(b). Separation increases in these cracks until the point of failure.

Cracking in the computer model starts in the elements surrounding the welded stud. In Figure 25 (b-d) the cracking continues along the area of the welded stud, and the elements beneath, and starts cracking in the grouted pocket. Toward the end of the analysis the majority of the multiple cracks that occur are around the welded plate and along the shear stud.

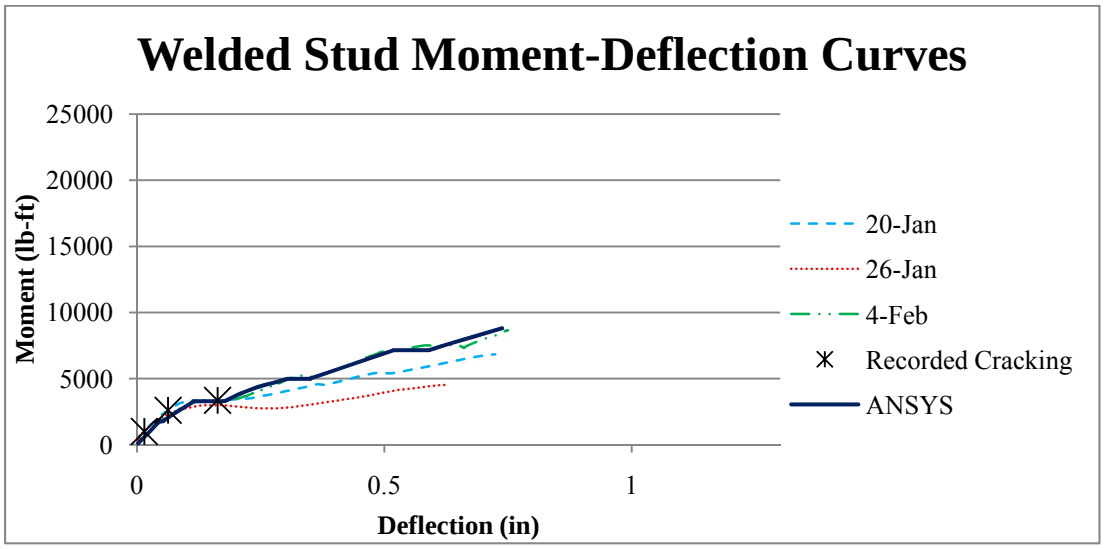

Figure 23. Welded stud moment-deflection curves.

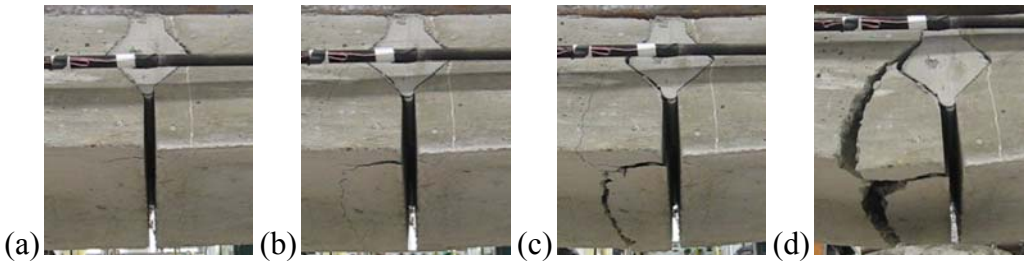

Figure 24. Flexural welded stud tested cracking sequence.

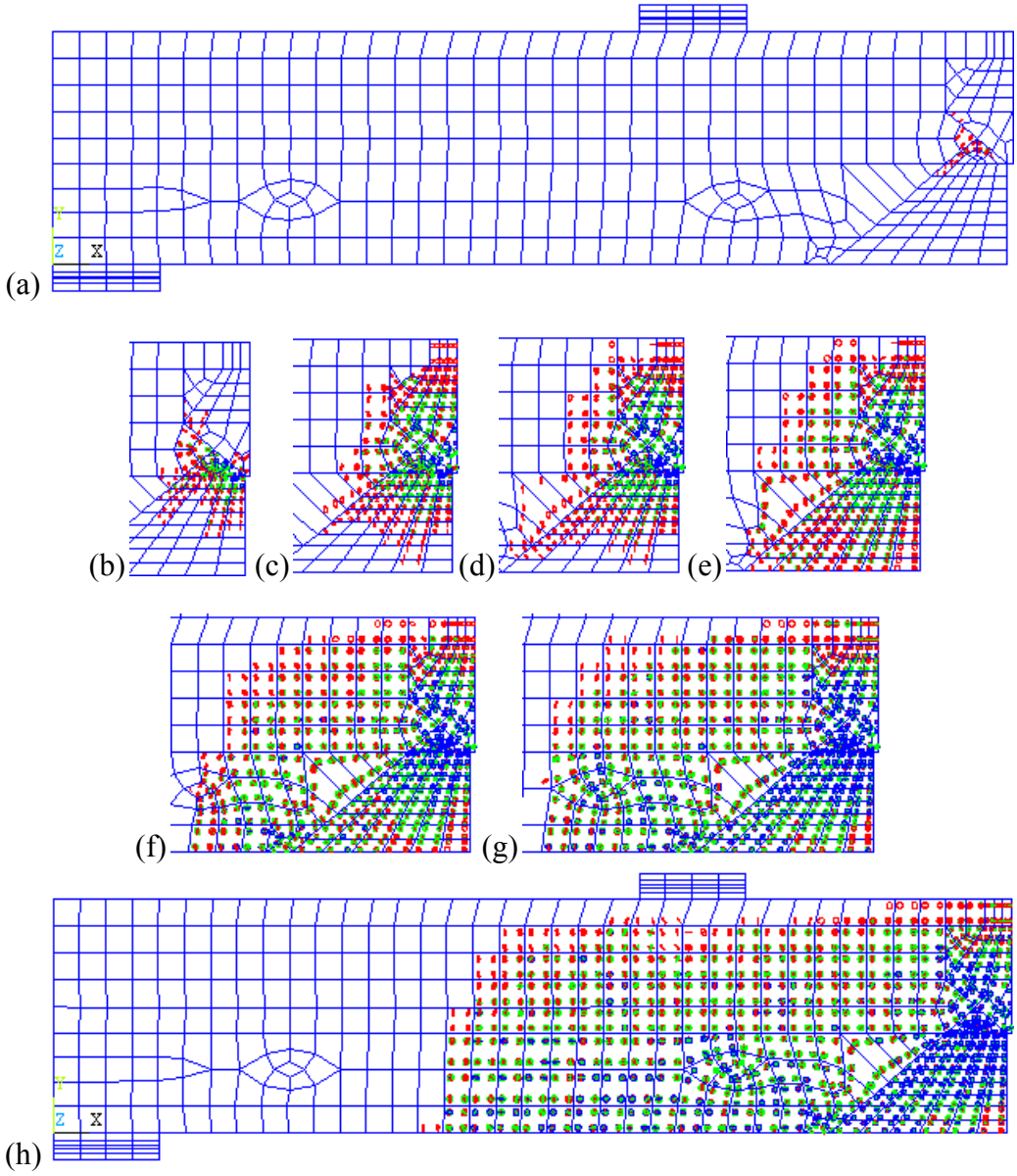

Figure 25. Flexural welded stud modeled cracking sequence.

Initial testing of the welded rebar modeled proved to produce a similar moment-deflection curve without using contact elements. This is due to a small linear region before cracking, where the finite element models proved to be much stiffer without the contact pairs. Surprisingly the initial cracking calculated in ANSYS occurs around 2,500

lb, while the recorded cracking during the laboratory testing occurs between 7,200 lb-ft to 13,700 lb-ft. A second point of major cracking with an increased deflection occurs at 11,059 lb-ft, which is within the range of the observed cracking. This second point of cracking is the small plateau seen in the ANSYS moment-deflection curve shown in Figure 26.

Cracking during testing for the welded rebar connection, shown in Figure 27, begins in the concrete at the bottom of the grouted pocket where connection plates are welded. Figure 27(b,c) shows the crack continue along the angle of the plate and into the concrete. Ultimate failure occurs at an angle that extends from the plate to the loading point. This cracking sequence is compared with the predicted cracking obtained from the finite element model shown in Figure 28. The cracking begins in the model near the corner of the welded plate between the concrete and grout. In Figure 28(b) multiple cracks occur along the angle of the plate, and the reinforcement. Multiple cracks follow

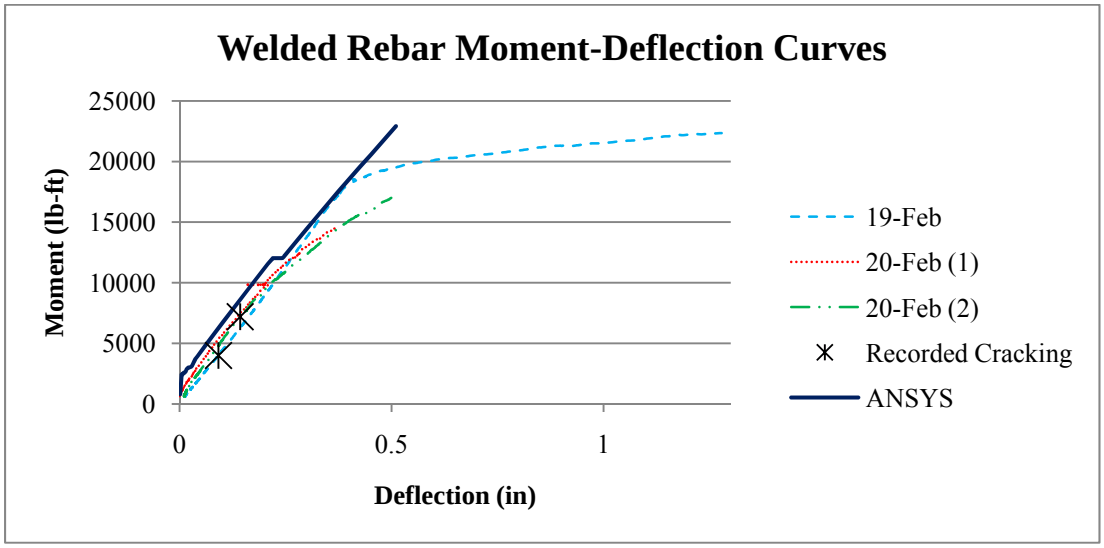

Figure 26. Welded rebar moment-deflection curves.

the welded rebar further into the concrete, and multiple cracks occur in the concrete in Figure 28(c-e).

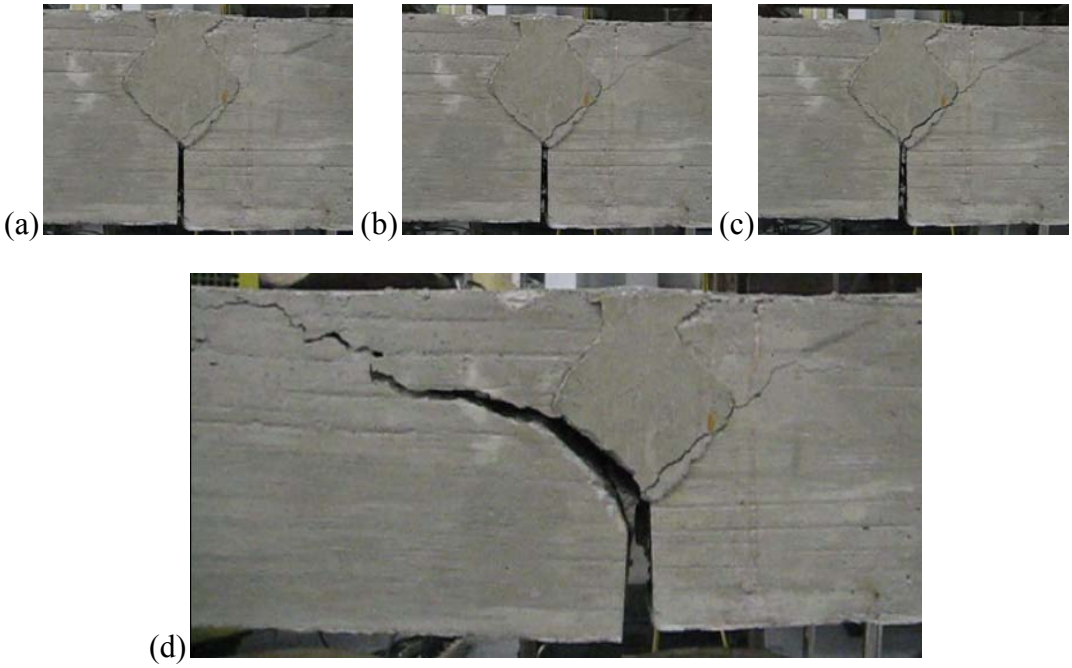

Figure 27. Flexural welded rebar tested cracking sequence.

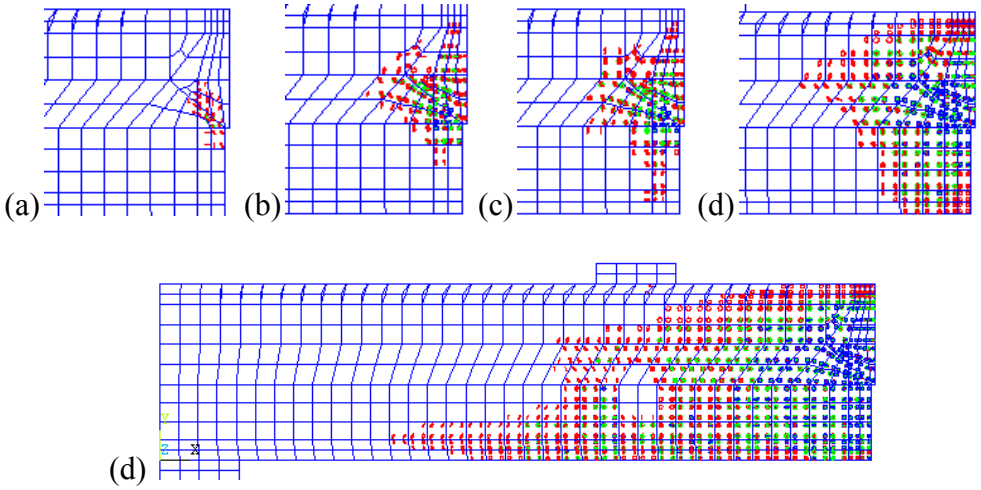

Figure 28. Flexural welded rebar modeled cracking sequence.

Initial analysis of the 36 inch curved bolt connection resulted in a moment-deflection curve that was extremely rigid until the point of cracking. After cracking the model deflected nearly 0.2 inches without additional load, and then followed the trend of the tested moment-deflection curve until termination of the analysis. The initial cracking moment was approximately 10,500 lb-ft. In an attempt to improve the results contact pairs were added along the concrete grout interface. The model with the added contact pairs had a similar curve to the tested specimen, but at the point of cracking the model deflected without added load, and resulted in a softer curve than the tested results. The final consideration in attempting to obtain accurate results was an assumption that the tested beams had cracking previous to testing. In order to model the beam being cracked, the model was loaded until the cracking moment, unloaded, and loaded to the full amount. The moment-deflection curves for the uncracked and cracked models are shown with the tested specimens in Figure 29. This shows that the curve of the cracked finite element model follows very closely to the tested results.

The cracking sequence for the tested specimen is illustrated in Figure 30, and shows the crack starting at the top corner of the grouted key below where the connection narrows. This crack continues roughly along the path of the curved bolt until the connection fails along the curved bolt region. The finite element cracking pattern is somewhat different, and could be accounted for by the way the curved bolt was modeled. In the tested specimen there was an oversized conduit, and when the tensile force was applied to the bolt it interacted with the conduit creating a vertical force as aforementioned. This may not be accurately represented in the ANSYS model because the curved bolt had direct contact with the concrete, and the tensile force was provided

due to thermal expansion. Cracking does occur in the model above the curved bolt at the final cracking stages, but initial cracking starts at the bottom of the beam below the left end of the curved bolt. Figure 31(a) shows the initial cracking around the curved bolt after the post tensioning is applied. The next cracking occurs at the mentioned location below the curved bolt. This spreads upwards through the thickness of the modeled deck. Cracking occurs at this location because after the curved bolt area is put into compression, this point has the highest tensile stresses.

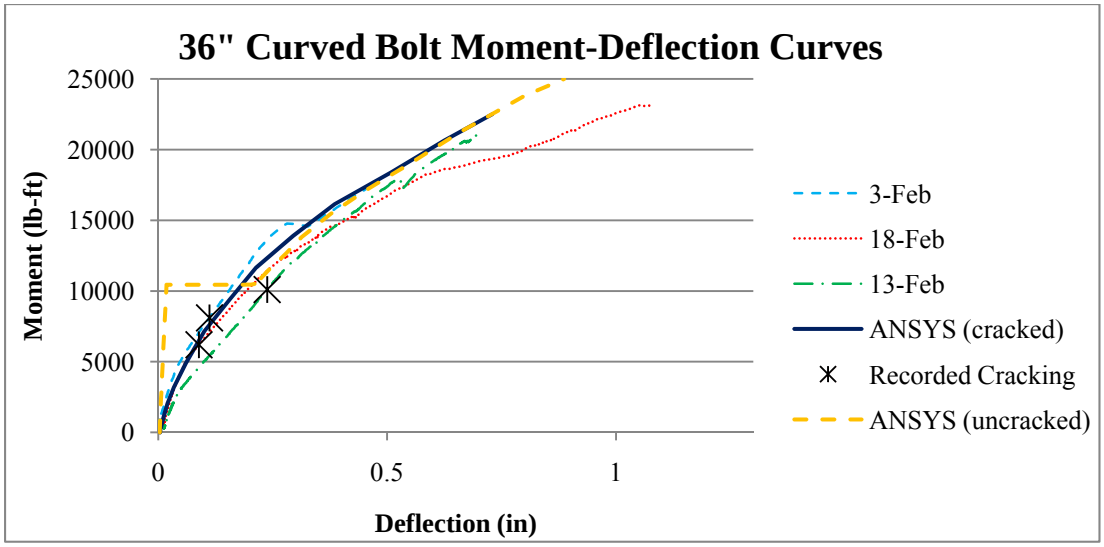

Figure 29. 36 inch curved bolt moment-deflection curves.

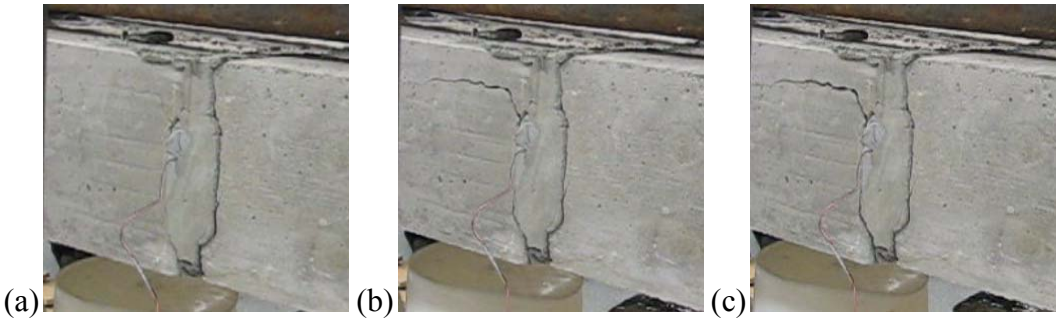

Figure 30. Flexural 36 inch curved bolt tested cracking sequence.

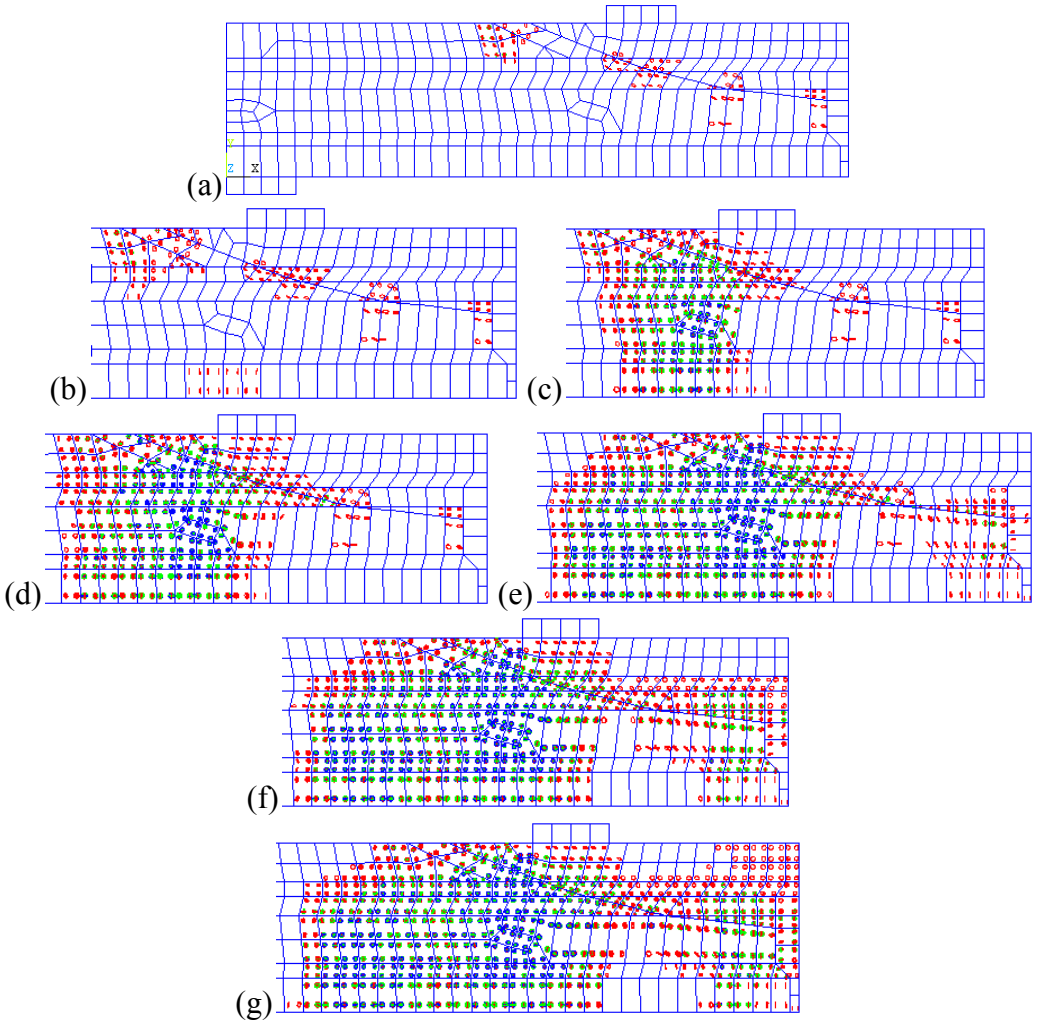

Figure 31. Flexural 36 inch curved bolt modeled cracking sequence.

The 24 inch curved bolt connection had a similar moment-deflection curve as the 36 inch for the modeled specimen. The initial slope for the linear region was very steep, and at cracking (approximately 9,000 lb-ft) the connection deflects significantly, and then follows the curve of the tested results. By using contact pairs the cracking moment was reduced to 8,700 lb-ft and more closely matched the tested results better. Similar to the 36 inch curved bolt connection the 24 inch connection was loaded to the cracking moment, unloaded, and loaded to the ultimate capacity. The moment-deflection curve

follows the tested specimen, as shown in Figure 32, but lacks the initial rigidity as shown in the tested specimens. The tested specimens initially have a rigid linear region, then around 3,000 to 4,000 lb-ft the deflection increases, and a more gradual curve follows. The modeled analysis does not show this trend.

The cracking sequence for the 24 inch curved bolt connection is similar to the 36 inch curved bolt, where a crack forms at the upper corner of the connection and follows the curved bolt conduit until failure. The cracking sequence is shown in Figure 32 and was compared to the ANSYS cracking predictions in Figure 34. The first cracks in ANSYS happen while the post tensioning is applied. These cracks occur around the curved bolt area, and when the full 300 psi is achieved across the connection the entire region above the curved bolt is shown as having initial cracking. After loading is applied the bottom of the beam directly below the end of the curved bolt. This can be assumed that comparable cracking will occur for curved bolt connection of varying curvatures.

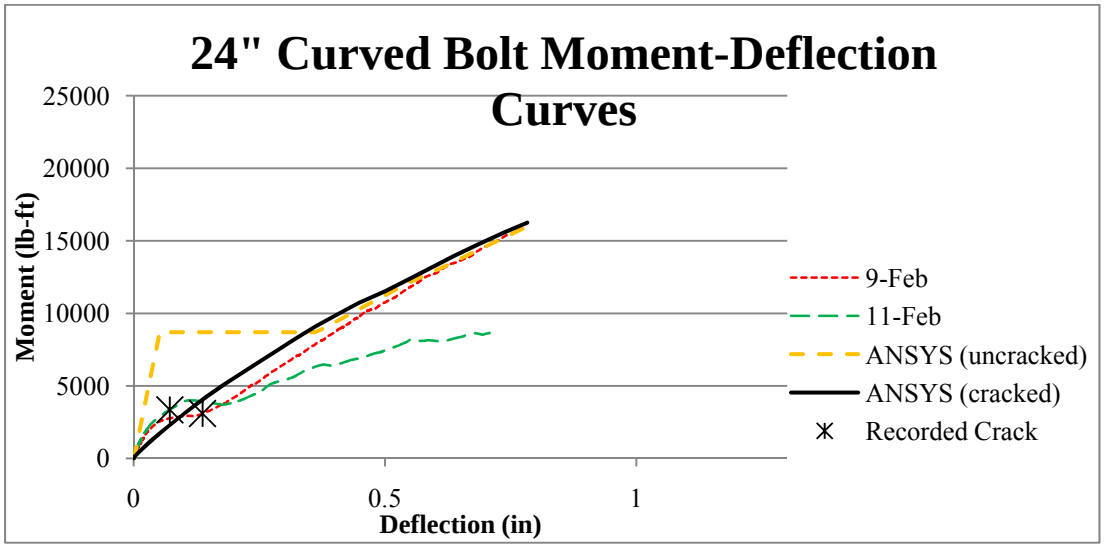

Figure 32. 24 inch curved bolt moment-deflection curves.

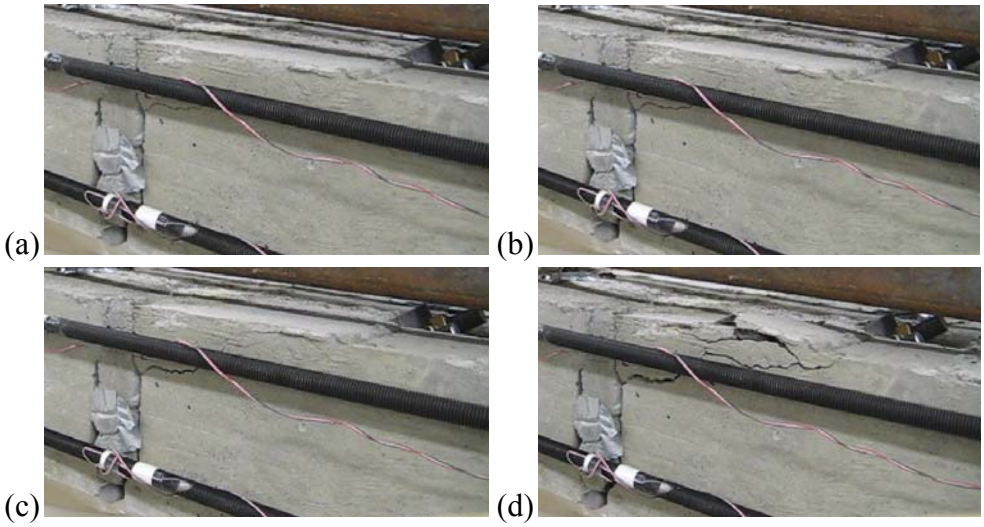

Figure 33. Flexural 24 inch curved bolt tested cracking sequence.

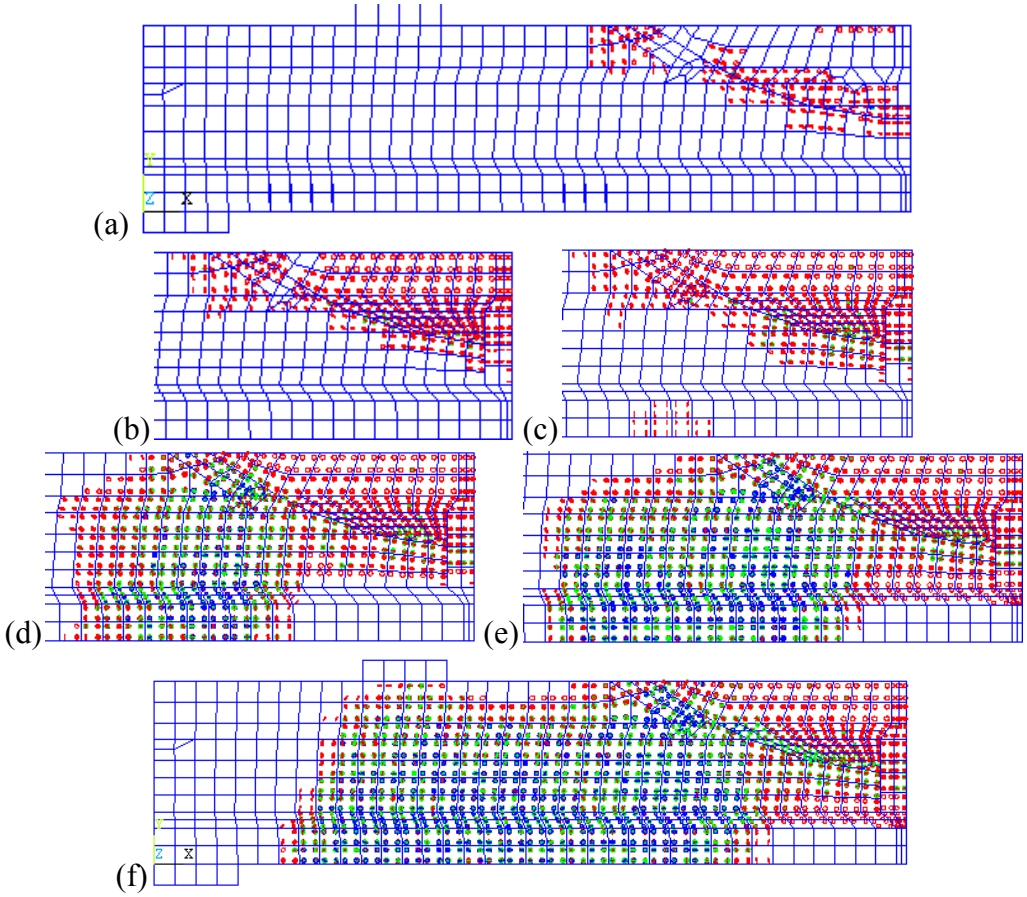

Figure 34. Flexural 24 inch curved bolt modeled cracking sequence.

CHAPTER VI

CONCLUSIONS

The four shear specimens modeled using ANSYS were: post tensioned, non-post tensioned, welded stud, and unreinforced section of the welded tie. The finite element models of the shear specimens showed similar results to tested models. For the non-post tensioned connection the cracking load predicted by ANSYS was within 10% of the average cracking load of the tested specimens. The location of the cracking was the same as the tested cracking pattern as was shown in Figures 9 and 10. The cracking load predicted in the finite element model of the unreinforced section of the welded tie was within 2% of the average cracking load for the tested results. The cracking load for the post tensioned model did not correlate well to the tested specimen cracking loads, however, the shear force-deflection curve matches the curve of the tested specimen results as was shown in Figure 17. Similarly the welded studs predicted cracking load does not have a good correlation with the tested results, but the force-deflection curve follows the curve of the tested results (Figure 11). All of the shear finite element models predicted the cracking location correctly. The shear force-deflection curves obtained from the finite element model closely follow the laboratory tested results. Because the shear finite element models for the non-post tensioned and unreinforced models for the non-post tensioned and unreinforced portion of the welded tie produced good results, they could be used in further analysis.

The five flexural models created in ANSYS were: post tensioned, 36 inch curved bolt, 24 inch curved bolt, welded stud, and welded rebar. Finite element analysis of

flexural models produced cracking moments, cracking locations, and moment-deflection curves that were similar to the laboratory tested results. The post tensioned model experienced a cracking moment that was within 10% of the highest observed cracking moment. The 36 inch curved bolt model predicted the cracking moment within 4% of the tested results. The cracking moment predicted by the 24 inch curved bolt model did not have a good correlation with the tested cracking moment, however the moment-deflecion curve follows the tested results as was shown by Figure 32.

Both welded tie models had initial cracking occurring within the model, and noticeable cracking that was referred to as a second crack. The moment at the second crack in both these models was close to the moment at the first cracks observed during testing. The welded stud had a predicted cracking moment that was within 2% of the largest observed cracking moment. The welded rebar had a predicted cracking moment that was within 20% of the largest observed cracking moment. Because the finite element model responded similarly to the test specimen, this indicates that internal cracking may occur in these models at relatively low loads. The models for the post tensioned, 36 inch curved bolt, welded stud, and welded rebar connections had accurate moment-deflection curves, and predicted cracking moment.

By observation of the tested specimens and finite element models in flexural, the internal cracking of the welded tie connections have a lower cracking moment, and ultimate strength depends more on the concrete strength. The connections with post tensioning crack at higher loads, and depend more on the bond strength between the concrete and grout.

Cracking resulted in the flanges of the shear specimens both in the laboratory testing and in the finite element model for post tensioned and welded stud connections. It is suggested for further research using similar shear models that the flange width and depth be increased. It is also suggested that the location where the deflection was recorded be moved to more accurately capture the connection deflection.

Simple forms of the curved bolt models were created in this analysis, and is suggested that the model could be improved by simulating the conduit for the curved bolt. An option for the curved bolt connection would be to place the curved bolt on the bottom of the section to avoid contact with the wearing surface. It is suggested that further analysis be performed with the curved bolt section on the bottom of the specimen.

Further analysis is recommended to find the ultimate strengths in ANSYS to compare with the laboratory tested results. Kachlakev (2001) determined the failure of the specimen at the point when convergence could no longer be reached after reducing the load substep to a 1 lb load increment. If the crushing capabilities were utilized ultimate loads might be determined.

It is suggested that the shear post tensioned, and shear welded stud models be improved to produce a more accurate cracking load. The model could also be improved to produce better load deflection behavior, possibly by modifying the contact pairs and CZM properties.

REFERENCES

ADINA R&D, Inc 1986. Watertown, MA.

ANSYS® Academic Research. 2007. Release 11.0, Help System, ANSYS, Inc.

Bakhoum, M. M. 1991. Shear behavior and design of joints in precast concrete segmental bridges. Unpublished PhD thesis. Massachusetts Institute of Technology, Cambridge. 153-191 p.

Biswas, M. 1986. Precast bridge deck design systems. PCI Journal 31(2), March-April, 40-94.

Computers and Structures. 1998. SAP2000 version 7.0: structural analysis program, Computers and Structures, Inc, Berkeley, California.

Issa, M. A., A. T. Idriss, I. I. Kaspar, and S. Y. Khayyat. 1995a. Full depth precast and precast, prestressed concrete bridge deck panels. PCI Journal 40(1), January-February, 59-80.

Issa M. A., A. A. Yousif, M. A. Issa, and S. Y. Khayyat. 1995b. Field performance of full depth precast concrete panels in bridge deck reconstruction. PCI Journal 40(3), May-June, 82-108.

Issa M. A., A. A. Yousif, and M. A. Issa. 1995. Construction procedures for rapid replacement of deteriorated bridge decks. Concrete International Journal 17(2), February, 49-52.

Issa, M. A., C. L. Ribiero do Valle, H. A. Abdalla, S. Islam, and M. A. Issa. 2003. Performance of transverse joint grout materials in full-depth precast concrete bridge deck systems. PCI Journal 48(4), July-August, 92-103.

Kachlakev, D., Miller T., and Yim, S. 2001. Finite element modeling of reinforced concrete structures strengthened with FRP laminates. Report for Oregon Department of Transportation, Salem.

Porter, S. 2009. Laboratory testing of precast bridge deck panel transverse connections for use in accelerated bridge construction. Unpublished Master's thesis. Utah State University, Logan.

Sullivan, S. 2007. Construction and behavior of precast bridge deck panel systems. Unpublished PhD dissertation. Virginia Polytechnic Institute and State University, Blacksburg.

Utah Department of Transportation. 2007. I-84: US-89 to SR-167, Weber Canyon. Bridge Deck Replacement Plans, UDOT Structures Division, Salt Lake City, Utah.

Utah Department of Transportation. 2008a. ABC standards. Full depth precast concrete deck panel standard drawings <http://www.dot.state.ut.us/main/uconowner.gf?n=1966945409050115798> (April 4, 2009), UDOT Structures Division, Salt Lake City, Utah.

Utah Department of Transportation. 2008b. Full depth precast concrete deck panel detailing manual. < http://www.dot.state.ut.us/main/f?p=100:pg:0::::T,V:2090,> (April 4, 2009) UDOT Structures Division, Salt Lake City, Utah.

Utah Department of Transportation. 2008c. Full depth concrete deck panels special provision. < http://www.dot.state.ut.us/main/f?p=100:pg:0::::T,V:2090,> (April 4, 2009) UDOT Structures Division, Salt Lake City, Utah.

Wolanski, A. J. 2004. Flexural behavior of reinforced and prestressed concrete beams using finite element analysis. Unpublished Master's thesis. Marquette University, Milwaulkee.

APPENDIX

SHEAR MODEL CODE

Key (Contact Elements)

```
finish
/clear
/title, Shear Unreinforced Key
/PREP7
!Steel area
area=0.2
! Concrete Elastic Modulus
Ec=3604997
Eg=4415201
! Concrete Poisson ratio
EMUc=0.2
! Concrete/Grout Compressive and Tensile Strength
fc=4000
fg=6000
ft=480
fy=60000
fgt=575
! Elastic Modulus and Poisson ratio for steel
Es=29e6
EMUs=0.3
! concrete element
ET,1,SOLID65
KEYOPT,1,3,2
KEYOPT,1,7,1
! steel element
ET,2,SOLID45
! rebar element
ET,3,LINK8
```

```
!Contact elements
Et,4,targe170
Et,5,conta173
Keyopt,5,10,2
Keyopt,5,2,1
Keyopt,5,12,5
Keyopt,5,9,1

! Real constants
R,1
R,2,area
R,3,.7854,!1.037e-3
R,4,,,.0011,,,,
R,5,,,.0011,,,,

MP,EX,1,Ec
MP,PRXY,1,EMUc
Mp,mu,1,.4
TB,CONC,1
TBDATA,,.2,.6,ft,-1,,

MP,EX,2,Es
MP,PRXY,2,EMUs
MP,EX,3,Es
MP,PRXY,3,EMUs
TB,BISO,3,,2
TBDAT,,fy,2900

MP,EX,4,Eg
MP,PRXY,4,EMUc
mp,ex,5,Ec

Mp,prxy,5,EMUc
```

```
TB,CONC,4,1,9,
TBDATA,,.2,.6,fgt,-1,,
Mp,ex,5,Ec
Mp,PRXY,5,EMUc

Tb,czm,6,1,1,CBDD
Tbdata,1,110,.015,,,.01,

K,1,
K,2,13
K,3,13,2
K,4,11,6
K,5,6.5,6
K,6,6.5,7
K,7,9.313,7
K,8,9.313,10.75
K,9,7,12.75
K,10,8.5,14.75
K,11,8.5,15.75
K,12,0,15.75
K,13,0,14.75
K,14,0,12.75
K,15,0,10.75
K,16,0,7
K,17,0,6
K,18,0,2
K,19,9.688,7
K,20,19.5,7
K,21,19.5,10.75
K,22,19.5,12.75
K,23,19.5,14.75
K,24,19.5,15.75
K,25,19.5,16.75
K,26,19.5,20.75
```

```
K,27,19.5,22.75
K,28,5,22.75
K,29,5,20.75
K,30,7,16.75
K,31,13,16.75
K,32,13,15.75
K,33,10.5,15.75
K,34,10.5,14.75
K,35,12,12.75
K,36,9.688,10.75

!Replicate Keypoints
KGEN,2,all,,,,,6
!Concrete volumes
V,1,37,38,2,18,54,39,3
V,18,54,39,3,17,53,40,4
V,17,53,41,5,16,52,42,6
V,16,52,43,7,15,51,44,8
V,15,51,44,8,14,50,45,9
V,14,50,45,9,13,49,46,10
V,13,49,46,10,12,48,47,11

V,19,55,56,20,36,72,57,21
V,36,72,57,21,35,71,58,22
V,35,71,58,22,34,70,59,23
V,34,70,59,23,33,69,60,24
V,32,68,60,24,31,67,61,25
V,30,66,61,25,29,65,62,26
V,29,65,62,26,28,64,63,27

!Grout Pocket
V,8,44,72,36,9,45,71,35
V,9,45,71,35,10,46,70,34
V,10,46,70,34,11,47,69,33
blc4,6.5,,6,-1,6
blc4,6.5,22.75,6,1,6

vsel,s,,,15,17
vgen,2,all,,,10,,,,,,0
vdele,15,17
vsel,s,,,20,22
vgen,,all,,,-10,,,,,1

vsel,s,,,1,7
vsel,a,,,18
vglue,all
vsel,s,,,20,22
vglue,all
vsel,s,,,8,14
vsel,a,,,19
vglue,all

Allsel,all
Esize,1

Lsel,s,,,169,172,3
Lesize,all,,,3

!—Mesh Grout
Vsel,s,,,20,22
Vatt,4,1,1
Vsweep,all
!—Mesh the Supports
Vsel,s,,,18,19
Vatt,2,1,2
Vsweep,all
!—Mesh Arms
vsel,s,,,2,4
vsel,a,,,15,17,2
vsel,a,,,12
vatt,5,1,1
vsweep,all
!—Mesh Concret
Vsel,s,,,18,22
vsel,a,,,2,4
vsel,a,,,12
vsel,a,,,15,17,2
Vsel,inve
Vatt,1,1,1
Vsweep,all
Allsel,all
Asel,s,,,45,55,5
Nsla,s,1
Type,4
Mat,1
Real,4
Esurf,,top
Allsel,all
Asel,s,,,102,112,5
Nsla,s,1
Type,5
Mat,6
Real,4
Tshape,quad
Esurf,,top

Allsel,all
Asel,s,,,100,110,5
Nsla,s,1
Type,4
Mat,1
Real,5
Esurf,,top
Allsel,all
Asel,s,,,26,36,5
Nsla,s,1
Type,5
Mat,6
Real,5
Tshape,quad
Esurf,,top

finish
/solu
!boundary conditions
allsel,all
asel,s,loc,x,19.5
nsla,s,1
d,all,ux
asel,s,loc,x
nsla,s,1
d,all,ux
asel,s,loc,z
nsla,s,1
d,all,uz
asel,s,loc,y,-1
nsla,s,1
d,all,uy

!apply force
Nsel,s,,,324,348
f,all,fy,-350
nsel,s,,,349,371
nsel,u,,,365,366
nsel,u,,,359
```

```
f,all,fy,-175
nsel,s,,,365,366
nsel,a,,,359,372,13
f,all,fy,-87.5

allsel,all
!—control parameters –
cnvtol,f,,0.05,2,.01
nsubst,50
outres,all,all
autots,1
ncnv,2
neqit,100
pred,on
time,100
 solve

!PT (CONTACT)

finish
/clear
/title, Shear PT
/PREP7
!Steel area
area=0.1
! Concrete Elastic Modulus
Ec=3604997
Eg=4415201
! Concrete Poisson ratio
EMUc=0.2
! Concrete Compressive
and Tensile Strength
fc=4000
fg=6000
ft=480
fy=60000
fgt=575
sc=.002219
sg=.002718
! Elastic Modulus and
Poisson ratio for steel
Es=29e6
EMUs=0.3
! concrete element
ET,1,SOLID65
KEYOPT,1,3,2
KEYOPT,1,7,1
! steel element
ET,2,SOLID45
! rebar element
ET,3,LINK8
! Real constants
Et,4,targe170
Et,5,conta173
Keyopt,5,10,2
Keyopt,5,2,1
Keyopt,5,12,5
Keyopt,5,9,1
Keyopt,5,5,1

R,1
R,2,area
R,3,.7854,!1.037e-3
MP,EX,1,Ec
MP,PRXY,1,EMUc
R,4,,,.0011,,,,
R,5,,,.0011,,,,
MP,EX,1,Ec
MP,PRXY,1,EMUc

TB,CONC,1
TBDATA,,.2,.6,ft,-1,,

MP,EX,2,Es
MP,PRXY,2,EMUs
MP,EX,3,Es
MP,PRXY,3,EMUs
TB,BISO,3,,2
TBDAT,,fy,2900

MP,EX,4,Eg
MP,PRXY,4,EMUc

TB,CONC,4,1,9,
TBDATA,,.2,.6,fgt,-1,,

MP,EX,5,Ec
MP,PRXY,5,EMUc
Tb,czm,6,1,1,CBDD
Tbdata,1,480,.015,,,.01,

K,1,
K,2,13
K,3,13,2
K,4,11,6
K,5,6.5,6
K,6,6.5,7
K,7,9,7
K,8,9,8.75
K,9,8.25,9.5
K,10,8.25,13
K,11,8.75,13.75
K,12,8.75,15.75
K,13,0,15.75
K,14,0,13.75
K,15,0,13
K,16,0,9.5
K,17,0,8.75
K,18,0,7
K,19,0,6
K,20,0,2
K,21,10,7
K,22,19.5,7
K,23,19.5,8.75
K,24,19.5,9.5
K,25,19.5,13
K,26,19.5,13.75
K,27,19.5,15.75
K,28,19.5,16.75
K,29,19.5,20.75
K,30,19.5,22.75
K,31,5,22.75
K,32,5,20.75
K,33,7,16.75
K,34,13,16.75
K,35,13,15.75
K,36,10.25,15.75
K,37,10.25,13.75
K,38,10.75,13
K,39,10.75,9.5
K,40,10,8.75
```

```
!Replicate Keypoints
KGEN,2,all,,,,,6

V,1,41,42,2,20,60,43,3
V,20,60,43,3,19,59,44,4
V,19,59,45,5,18,58,46,6
V,18,58,47,7,17,57,48,8
V,17,57,48,8,16,56,49,9
V,16,56,49,9,15,55,50,10
V,15,55,50,10,14,54,51,11
V,14,54,51,11,13,53,52,12

V,21,61,62,22,40,80,63,23
V,40,80,63,23,39,79,64,24
V,39,79,64,24,38,78,65,25
V,38,78,65,25,37,77,66,26
V,37,77,66,26,36,76,67,27
V,35,75,67,27,34,74,68,28
V,33,73,68,28,32,72,69,29
V,32,72,69,29,31,71,70,30

!Grout Pocket
V,7,47,61,21,8,48,80,40
V,8,48,80,40,9,49,79,39
V,9,49,79,39,10,50,78,38
V,10,50,78,38,11,51,77,37
V,11,51,77,37,12,52,76,36
blc4,6.5,,6,-1,6
blc4,6.5,22.75,6,1,6

vsel,s,,,17,21
vgen,2,all,,,10,,,,,,0
vdele,17,21
vsel,s,,,24,28
vgen,,all,,,-10,,,,,1

vsel,s,,,1,8
vsel,a,,,22
vglue,all
vsel,s,,,24,28
vglue,all
vsel,s,,,9,16
vsel,a,,,23
vglue,all

Allsel,all
Esize,1

!--Mesh Grout
Vsel,s,,,24,28
Vatt,4,1,1
Vsweep,all
!--Mesh the Supports
Vsel,s,,,22,23
Vatt,2,1,2
Vsweep,all

!—Mesh RC
vsel,s,,,2,4
vsel,a,,,14,17,3
vsel,a,,,19
vatt,5,1,1
vsweep,all
!--Mesh Concret
Vsel,s,,,22,28
Vsel,a,,,2,4
vsel,a,,,14,17,3
vsel,a,,,19
Vsel,inve
Vatt,1,1,1
Vsweep,all

Allsel,all
Asel,s,,,45,65,5
!Asel,s,,,118,138,5
Nsla,s,1
Type,4
Mat,1
Real,4
Esurf,,top
Allsel,all
Asel,s,,,118,138,5
!Asel,s,,,45,65,5
Nsla,s,1
Type,5
Mat,6
Real,4
Tshape,quad
Esurf,,top

Allsel,all
Asel,s,,,21,41,5
!Asel,s,,,116,136,5
Nsla,s,1
Type,4
Mat,1
Real,5
Esurf,,top
Allsel,all
Asel,s,,,116,136,5
!Asel,s,,,21,41,5
Nsla,s,1
Type,5
Mat,6
Real,5
Tshape,quad
Esurf,,top

finish
/solu
!boundary conditions
allsel,all
asel,s,loc,x,19.5
nsla,s,1
d,all,ux
asel,s,loc,z
nsla,s,1
d,all,uz
asel,s,loc,y,-1
nsla,s,1
d,all,uy

apply pressure
Asel,s,loc,x
Asel,u,,,2,7
Asel,u,,,13
!Asel,a,loc,x,19.5
!Asel,u,,,73,79,6
!Asel,u,,,84
sfa,all,1,pres,300

allsel,all
!—control parameters –
cnvtol,f,,0.05,2,.01
nsubst,25
```

```
outres,all,all
autots,1
ncnv,2
neqit,50
pred,on
time,50
 solve

!apply force
Nsel,s,,,352,376
f,all,fy,-600
nsel,s,,,377,400
nsel,u,,,393,394
nsel,u,,,387,400,13
f,all,fy,-300
nsel,s,,,393,394
nsel,a,,,387,400,13
f,all,fy,-100

allsel,all
!—control parameters –
cnvtol,f,,0.05,2,.01
nsubst,50
outres,all,all
autots,1
ncnv,2
neqit,100
pred,on
time,100
 solve
```

!Welded Connections (Contact)

```
finish
/clear
/title, Shear Welded Stud
/PREP7
!Steel area
area=0.2
! Concrete Elastic Modulus
Ec=3604997
Eg=4415201
! Concrete Poisson ratio
EMUc=0.2
! Concrete Compressive
and Tensile Strength
fc=4000
fg=6000
ft=480
fy=60000
fgt=575
sc=.002585
sg=.002743
! Elastic Modulus and
Poisson ratio for steel
Es=29e6
EMUs=0.3
! concrete element
ET,1,SOLID65
KEYOPT,1,3,2
KEYOPT,1,7,1
! steel element
ET,2,SOLID45
! rebar element
ET,3,LINK8
Et,4,targe170
Et,5,conta173
Keyopt,5,10,2
Keyopt,5,2,1
Keyopt,5,12,5
Keyopt,5,9,1
Keyopt,5,5,1

! Real constants
R,1
R,2,area
R,3,1.227,!1.037e-3
R,4,,,.0011,,,,
R,5,,,.0011,,,,
MP,EX,1,Ec
MP,PRXY,1,EMUc
Mp,mu,1,.5

TB,CONC,1
TBDATA,,.2,.6,ft,-1,,

MP,EX,2,Es
MP,PRXY,2,EMUs
MP,EX,3,Es
MP,PRXY,3,EMUs
TB,BISO,3,,2
TBDAT,,fy,2900

MP,EX,4,Eg
MP,PRXY,4,EMUc

TB,CONC,4,1,9,
TBDATA,,.2,.6,fgt,-1,,
Mp,ex,5,Ec
Mp,prxy,5,EMUc

Tb,czm,6,1,1,CBDD
Tbdata,1,480,.015,,,.01,

K,1,
K,2,13
K,3,13,2
K,4,11,6
K,5,6.5,6
K,6,6.5,7
K,7,9.313,7
K,8,9.313,10.75
K,9,7,12.75
K,10,7,15.75
K,11,0,15.75
K,12,0,12.75
K,13,0,10.75
K,14,0,7
K,15,0,6
K,16,0,2
K,17,9.688,7
K,18,19.5,7
K,19,19.5,10.75
K,20,19.5,12.75
K,21,19.5,15.75
K,22,19.5,16.75
K,23,19.5,18.75
K,24,19.5,20.813
K,25,19.5,24.75
K,26,5,24.75
K,27,5,20.813
K,28,6,18.75
K,29,11,18.75
```

```
K,30,13,16.75
K,31,13,15.75
K,32,12,15.75
K,33,12,12.75
K,34,9.688,10.75

!Replicate Keypoints
KGEN,2,all,,,,,2

V,1,35,36,2,16,50,37,3
V,16,50,37,3,15,49,38,4
V,15,49,39,5,14,48,40,6
V,14,48,41,7,13,47,42,8
V,13,47,42,8,12,46,43,9
V,12,46,43,9,11,45,44,10

V,17,51,52,18,34,68,53,19
V,34,68,53,19,33,67,54,20
V,33,67,54,20,32,66,55,21
V,31,65,55,21,30,64,56,22
V,30,64,56,22,29,63,57,23
V,28,62,57,23,27,61,58,24
V,27,61,58,24,26,60,59,25

!Grout Pocket
V,8,42,68,34,9,43,67,33
V,9,43,67,33,10,44,66,32

Vgen,3,all,,,,,2

blc4,6.5,,6,-1,6
blc4,6.5,24.75,6,1,6

wpoff,7,10.75
wprot,40.85537626,90
Vsel,s,,,4,5
Vsel,a,,,19,20
Vsel,a,,,34,35
vsbw,all
wprot,0,-90
wprot,-40.85537626
wpoff,5
wprot,-40.85537626,90
vsel,s,,,7,8
vsel,a,,,22,23
vsel,a,,,37,38
vsbw,all
wprot,0,-90
wprot,40.85537626
wpoff,0,-2.75
wprot,0,90
allsel,all
vsbw,all

vsel,s,,,14,15
vsel,a,,,29,30
vsel,a,,,44,45
vgen,2,all,,,10,,,,,,0
vsel,s,,,14,15
vsel,a,,,29,30
vsel,a,,,44,45
vdele,all
vsel,s,,,20
vsel,a,,,34,35
vsel,a,,,51,53
vgen,,all,,,-10,,,,,1

vsel,s,,,20
vsel,a,,,34,35
vsel,a,,,51,53
vglue,all

vsel,s,,,1,3
vsel,a,,,6,21,15
vsel,a,,,16,18
vsel,a,,,31,33
vsel,a,,,36,38,2
vsel,a,,,46
vsel,a,,,48,50
vsel,a,,,57,59
vsel,a,,,66,70
vsel,a,,,71,76
vglue,all
vsel,s,,,4,5
vsel,a,,,7,13
vsel,a,,,19
vsel,a,,,22,28
vsel,a,,,37,47,10
vsel,a,,,39,43
vsel,a,,,63,65
vsel,a,,,77,83
vglue,all
!glue plate and stud
Lsel,s,,,49,71,22
Lsel,a,,,176,200,24
Lsel,a,,,420,425,5
Lsel,a,,,531,537,6
Lsel,a,,,35,41,2
Lsel,a,,,63,69,2
Lsel,a,,,165,167,2
Lsel,a,,,168,171,3
Lsel,a,,,195,196
Lsel,a,,,199,295,96
Lsel,a,,,454,479,25
Lsel,a,,,497
Lsel,a,,,607,608
Lsel,a,,,624,633,3
Lsel,a,,,634
Lsel,a,,,649,650
Lsel,a,,,653,654
Lsel,a,,,657,664
Lglue,all

allsel,all
Esize,1

!--Mesh Concret
Vsel,s,,,14,15
Vsel,a,,,29,30
Vsel,a,,,20,34,14
Vsel,a,,,10,11
Vsel,a,,,17,18
Vsel,a,,,21,31,10
Vsel,a,,,61,62
Vsel,a,,,71,76,5
Vsel,a,,,73,74
Vsel,a,,,87,90
Vsel,a,,,95,97
Vsel,a,,,59,93,34
Vsel,a,,,75,94,19
Vsel,inve
Vatt,1,1,1
Vsweep,all

!--Mesh Grout
```

```
Vsel,s,,,14,15
Vsel,a,,,29,30
Vsel,a,,,20,34,14
Vatt,4,1,1
Vsweep,all
!--Mesh the Supports
Vsel,s,,,75,94,19
Vatt,2,1,2
Vsweep,all
!—Mesh NoCrack
Vsel,s,,,10,11
Vsel,a,,,17,18
Vsel,a,,,21,31,10
Vsel,a,,,61,62
Vsel,a,,,71,76,5
Vsel,a,,,73,74
Vsel,a,,,87,90
Vsel,a,,,95,97
Vsel,a,,,59,93,34
Vatt,5,1,1
Vsweep,all

!Mesh rebar
Lsel,s,,,49,71,22
Lsel,a,,,176,200,24
Lsel,a,,,82
Lsel,a,,,425
Lsel,a,,,531,537,6
Latt,3,2,3
Lmesh,all
!mesh plate
Lsel,s,,,35,41,2
Lsel,a,,,63,69,2
Lsel,a,,,86
Lsel,a,,,107,108
Lsel,a,,,120,124,4
Lsel,a,,,165,167,2
Lsel,a,,,179,189,10
Lsel,a,,,191,195,4
Lsel,a,,,198,203,5
Lsel,a,,,206,295,89
Lsel,a,,,454
Lsel,a,,,196
Lsel,a,,,624,633,3
Lsel,a,,,634,649,15
Lsel,a,,,650,662,4
Lsel,a,,,653,661,4
Latt,3,3,3
Lmesh,all
Allsel,all
Asel,s,,,21,35,14
Asel,a,,,175,310,135
Asel,a,,,399,409,5
Asel,a,,,403,408,5
Nsla,s,1
Type,4
Mat,1
Real,4
Esurf,,top
Allsel,all
Asel,s,,,31,191,160
Asel,a,,,250,266,16
Asel,a,,,276,286,5
Asel,a,,,429,431,2
Nsla,s,1
Type,5
Mat,6
Real,4
Tshape,quad
Esurf,,top

Allsel,all
Asel,s,,,97,99,2
Asel,a,,,177,312,135
Asel,a,,,400,410,5
Asel,a,,,406,411,5
Nsla,s,1
Type,4
Mat,1
Real,5
Esurf,,top
Allsel,all
Asel,s,,,3,10,7
Asel,a,,,23,45,22
Asel,a,,,173,185,12
Asel,a,,,189,261,72
Asel,a,,,313
Nsla,s,1
Type,5
Mat,6
Real,5
Tshape,quad
Esurf,,top
finish
/solu
!boundary conditions
allsel,all
asel,s,loc,x,19.5
nsla,s,1
d,all,ux
asel,s,loc,x
nsla,s,1
d,all,ux
asel,s,loc,z
nsla,s,1
d,all,uz
asel,s,loc,y,-1
nsla,s,1
d,all,uy

!apply force
Nsel,s,,,2092,2116
f,all,fy,-600
nsel,s,,,2081,2091
nsel,a,,,2010,2014
nsel,a,,,2117,2121
nsel,u,,,2086
f,all,fy,-300
nsel,s,,,2080,2086,6
nsel,a,,,2015,2016
f,all,fy,-150

allsel,all
!—control parameters –
cnvtol,f,,0.05,2,.01
nsubst,100
outres,all,all
autots,1
ncnv,2
neqit,200
pred,on
time,50
 solve
```

```
!No PT (Contact)

finish
/clear
/title, Shear PT
/PREP7
!Steel area
area=0.1
! Concrete Elastic Modulus
Ec=3604997
Eg=4415201
! Concrete Poisson ratio
EMUc=0.2
! Concrete Compressive
and Tensile Strength
fc=4000
fg=6000
ft=480
fy=60000
fgt=575
sc=.002219
sg=.002718
! Elastic Modulus and
Poisson ratio for steel
Es=29e6
EMUs=0.3
! concrete element
ET,1,SOLID65
KEYOPT,1,3,2
KEYOPT,1,7,1
! steel element
ET,2,SOLID45
! rebar element
ET,3,LINK8
! Real constants
Et,4,targe170
Et,5,conta173
Keyopt,5,10,2
Keyopt,5,2,1
Keyopt,5,12,5
Keyopt,5,9,1
Keyopt,5,5,1

R,1
R,2,area
R,3,.7854,!1.037e-3
MP,EX,1,Ec
MP,PRXY,1,EMUc
R,4,,,.0011,,,,
R,5,,,.0011,,,,
MP,EX,1,Ec
MP,PRXY,1,EMUc
Mp,mu,1,.5

TB,CONC,1
TBDATA,,.2,.6,ft,-1,,

MP,EX,2,Es
MP,PRXY,2,EMUs
MP,EX,3,Es
MP,PRXY,3,EMUs
TB,BISO,3,,2
TBDAT,,fy,2900

MP,EX,4,Eg
MP,PRXY,4,EMUc

TB,CONC,4,1,9,
TBDATA,,.2,.6,fgt,-1,,

MP,EX,5,Ec
MP,PRXY,5,EMUc

Tb,czm,6,1,1,CBDD
Tbdata,1,480,.015,,,.01,

K,1,
K,2,13
K,3,13,2
K,4,11,6
K,5,6.5,6
K,6,6.5,7
K,7,9,7
K,8,9,8.75
K,9,8.25,9.5
K,10,8.25,13
K,11,8.75,13.75
K,12,8.75,15.75
K,13,0,15.75
K,14,0,13.75
K,15,0,13
K,16,0,9.5
K,17,0,8.75
K,18,0,7
K,19,0,6
K,20,0,2
K,21,10,7
K,22,19.5,7
K,23,19.5,8.75
K,24,19.5,9.5
K,25,19.5,13
K,26,19.5,13.75
K,27,19.5,15.75
K,28,19.5,16.75
K,29,19.5,20.75
K,30,19.5,22.75
K,31,5,22.75
K,32,5,20.75
K,33,7,16.75
K,34,13,16.75
K,35,13,15.75
K,36,10.25,15.75
K,37,10.25,13.75
K,38,10.75,13
K,39,10.75,9.5
K,40,10,8.75

!Replicate Keypoints
KGEN,2,all,,,,,6

V,1,41,42,2,20,60,43,3
V,20,60,43,3,19,59,44,4
V,19,59,45,5,18,58,46,6
V,18,58,47,7,17,57,48,8
V,17,57,48,8,16,56,49,9
V,16,56,49,9,15,55,50,10
V,15,55,50,10,14,54,51,11
V,14,54,51,11,13,53,52,12

V,21,61,62,22,40,80,63,23
V,40,80,63,23,39,79,64,24
V,39,79,64,24,38,78,65,25
V,38,78,65,25,37,77,66,26
V,37,77,66,26,36,76,67,27
V,35,75,67,27,34,74,68,28
```

```
V,33,73,68,28,32,72,69,29
V,32,72,69,29,31,71,70,30

!Grout Pocket
V,7,47,61,21,8,48,80,40
V,8,48,80,40,9,49,79,39
V,9,49,79,39,10,50,78,38
V,10,50,78,38,11,51,77,37
V,11,51,77,37,12,52,76,36
blc4,6.5,,6,-1,6
blc4,6.5,22.75,6,1,6

vsel,s,,,17,21
vgen,2,all,,,10,,,,,,0
vdele,17,21
vsel,s,,,24,28
vgen,,all,,,-10,,,,,1

vsel,s,,,1,8
vsel,a,,,22
vglue,all
vsel,s,,,24,28
vglue,all
vsel,s,,,9,16
vsel,a,,,23
vglue,all

Allsel,all
Esize,1

!--Mesh Grout
Vsel,s,,,24,28
Vatt,4,1,1
Vsweep,all
!--Mesh the Supports
Vsel,s,,,22,23
Vatt,2,1,2
Vsweep,all

!—Mesh RC
vsel,s,,,2,4
vsel,a,,,14,17,3
vsel,a,,,19
vatt,5,1,1
vsweep,all

!--Mesh Concret
Vsel,s,,,22,28
Vsel,a,,,2,4
vsel,a,,,14,17,3
vsel,a,,,19
Vsel,inve
Vatt,1,1,1
Vsweep,all

Allsel,all
Asel,s,,,118,138,5
Nsla,s,1
Type,4
Mat,1
Real,4
Esurf,,top
Allsel,all
Asel,s,,,45,65,5
Nsla,s,1
Type,5
Mat,6
Real,4
Tshape,quad
Esurf,,top

Allsel,all
Asel,s,,,116,136,5
Nsla,s,1
Type,4
Mat,1
Real,5
Esurf,,top
Allsel,all
Asel,s,,,21,41,5
Nsla,s,1
Type,5
Mat,6
Real,5
Tshape,quad
Esurf,,top

finish
/solu
!boundary conditions
allsel,all
asel,s,loc,x,19.5
nsla,s,1
d,all,ux
asel,s,loc,x
nsla,s,1
d,all,ux,!.0015
asel,s,loc,z
nsla,s,1
d,all,uz
asel,s,loc,y,-1
nsla,s,1
d,all,uy

!apply force
Nsel,s,,,352,376
f,all,fy,-215
nsel,s,,,377,400
nsel,u,,,393,394
nsel,u,,,387,400,13
f,all,fy,-107.5
nsel,s,,,393,394
nsel,a,,,387,400,13
f,all,fy,-53.75

allsel,all
!—control parameters –
cnvtol,f,,0.05,2,.01
nsubst,50
outres,all,all
autots,1
ncnv,2
neqit,100
pred,on
time,100
 solve
```

FLEXURAL MODEL CODE

```
finish
/clear
/title, Welded Rebar
/PREP7
!Steel area
area=0.44
! Concrete Elastic Modulus
Ec=3604997
Eg=4415201
! Concrete Poisson ratio
EMUc=0.2
! Concrete/Grout
compressive and tensile
strength
fc=4000
fg=6000
ft=480
fy=60000
fgt=575
! Elastic modulus and
Poisson ratio for steel
Es=29e6
EMUs=0.3
! concrete element
ET,1,SOLID65
KEYOPT,1,3,2
KEYOPT,1,7,1
! steel element
ET,2,SOLID45
! rebar element
ET,3,LINK8
! Real constants
R,1,3,0.0075,0,90,3,.0075,
RMORE,90, , , , , ,
R,2,area
R,3,.7934 !1.227
R,4
MP,EX,1,Ec
MP,PRXY,1,EMUc
```

Rebar Code (Contact)

```
TB,CONC,1
TBDATA,,.9,1,ft,-1,,

MP,EX,2,Es
MP,PRXY,2,EMUs
MP,EX,3,Es
MP,PRXY,3,EMUs
TB,BISO,3,,2
TBDAT,,fy,2900

MP,EX,4,Eg
MP,PRXY,4,EMUc

TB,CONC,4,1,9,

TBDATA,,.9,.1,fgt,-1,,

!add all keypoints
K,1,
K,2,35.8125
K,3,35.8125,3.75
K,4,33.5,5.75
K,5,35,7.75
K,6,35,8.75
K,7,33.5,8.75
K,8,0,8.75
K,9,0,7.75
K,10,0,5.75
K,11,0,3.75
K,12,33.5,7.75
K,13,36
K,14,36,3.75
K,15,36,5.75
K,16,36,7.75
K,17,36,8.75

!Replicate Keypoints
KGEN,2,all,,,,,3
KGEN,2,1,17,,,,9
```

```
!Create volumes through
keypoints
V,1,18,19,2,11,28,20,3
V,11,28,20,3,10,27,21,4
V,10,27,21,4,9,26,29,12
V,9,26,29,12,8,25,24,7
V,4,21,22,5,7,24,23,6

V,3,20,31,14,4,21,32,15
V,4,21,32,15,5,22,33,16
V,5,22,33,16,6,23,34,17

V,18,35,36,19,28,45,37,20
V,28,45,37,20,27,44,38,21
V,27,44,38,21,26,43,46,29
V,26,43,46,29,25,42,41,24
V,21,38,39,22,24,41,40,23

V,20,37,48,31,21,38,49,32
V,21,38,49,32,22,39,50,33
V,22,39,50,33,23,40,51,34
blc4,,,4,-1,9
blc4,22,8.75,4,1,9
wpoff,0,0,1.5
vsbw,all
wpoff,0,0,4.5
vsbw,all
wpoff,0,1
wprot,0,90
vsbw,all
wpoff,0,0,-6.75
vsbw,all
wpoff,34.65625
wprot,0,-90,90
vsel,s,,,21,22
vsel,a,,,18,42,24
vsel,a,,,29,30
vsel,a,,,2,6,4
vsel,a,,,9,16
vsbw,all
```

```
wpstyl
allsel,all
vglue,all
Nummrg,all
numcmp,all

Lsel,s,,,2,9,7
Lsel,a,,,59,97,38
Lsel,a,,,109,116,7
Lsel,a,,,169,187,18
Lsel,a,,,193,215,22
Lsel,a,,,197,207,5
Lsel,a,,,209,210
Lsel,a,,,221,226,5
Lsel,a,,,229
Lesize,all,.75

DESIZE,2,2,9999,15,28,1,2
,1,4

!Mesh Grout
Vsel,s,,,5,6
Vsel,a,,,15,17,2
Vsel,a,,,21,37,16
Vsel,a,,,24,27
Vsel,a,,,31,56,25
Vsel,a,,,33,34
Vsel,a,,,39
Vsel,a,,,40,42,2
Vsel,a,,,59,60
Vsel,a,,,62
Vatt,4,4,1
!Mopt,pyra,off
!Mshkey,1
!MSHAPE,0,3D
!DESIZE,1,1,9999,15,28,1,
2,1,4
Vsweep,all

!Mesh Plate
Lsel,s,,,32
Lsel,a,,,38,40,2
Lsel,a,,,113,118,5
Lsel,a,,,121,125,4
Lsel,a,,,142,143
Lsel,a,,,147,250,103
Lsel,a,,,258,261,3
Lsel,a,,,263,266,3
Lsel,a,,,267,271,4
Latt,3,3,3
Lmesh,all

!Mesh Concrete
Vsel,s,,,5,6
Vsel,a,,,15,17,2
Vsel,a,,,21,37,16
Vsel,a,,,24,27
Vsel,a,,,31,56,25
Vsel,a,,,33,34
Vsel,a,,,39
Vsel,a,,,40,42,2
Vsel,a,,,59,60
Vsel,a,,,62
Vsel,a,,,10,11
Vsel,a,,,28,30,2
Vsel,a,,,35,36
Vsel,inve
Vatt,1,1,1
Vsweep,all

!Mesh Welded Rebar
Lsel,s,,,35,249,214
Lsel,a,,,253,264,11
Lsel,a,,,307,313,6
Latt,3,2,3
Lmesh,all

!Mesh Supports
Vsel,s,,,10,11
Vsel,a,,,28,30,2
Vsel,a,,,35,36
Vatt,2,,2
Vsweep,all

Nummrg,all
Numcmp,all

finish
/solu
!boundary conditions
allsel,all
asel,s,loc,x,36
nsla,s,1
d,all,ux
asel,s,loc,z
nsla,s,1
d,all,uz

nsel,s,,,6416
Nsel,a,,,6273,6275
Nsel,a,,,6321,6325
Nsel,a,,,6338,6342,4
Nsel,a,,,6265,6376,111
D,all,UY

Nsel,none
Nsel,s,,,6442
F,all,fy,-300
Nsel,none
Nsel,s,,,6282,6284
Nsel,a,,,6349,6353
Nsel,a,,,6268,6394,126
Nsel,a,,,6366,6369,3
Nsel,a,,,6268
F,all,FY,-600

allsel,all
!—control parameters –
cnvtol,f,,0.05,2,.01
nsubst,50
outres,all,all
autots,1
ncnv,2
neqit,100
pred,on
time,50
solve

!Post Tensioned(Contact)

finish
/clear
/title, Post Tension
/PREP7
```

```
!Steel area
area=0.44
! Concrete Elastic Modulus
Ec=3605000
Eg=4415201
! Concrete Poisson ratio
EMUc=0.2
! Concrete Compressive
and Tensile Strength
fc=4000
fg=6000
ft=480
fy=60000
fgt=575
sc=.002585
sg=.002743
! Elastic Modulus and
Poisson ratio for steel
Es=29e6
EMUs=0.3
! concrete element
ET,1,SOLID65
KEYOPT,1,3,2
KEYOPT,1,7,1
! steel element
ET,2,SOLID45
! rebar element
ET,3,LINK8
Et,4,targe170
Et,5,conta173
Keyopt,5,10,2
Keyopt,5,2,1
Keyopt,5,12,5
Keyopt,5,9,1
Keyopt,5,5,1

! Real constants
R,1,3,.002,90,3,.002,0,
RMORE,90, , , , , ,
R,2,area
R,3,.44,9.22e-4
R,4,,,.0036,,,,
r,5
```

```
MP,EX,1,Ec
MP,PRXY,1,EMUc

TB,CONC,1
TBDATA,,.2,.6,ft,-1,,

MP,EX,2,Es
MP,PRXY,2,EMUs
MP,EX,3,Es
MP,PRXY,3,EMUs
TB,BISO,3,,2
TBDAT,,fy,2900

MP,EX,4,Eg
MP,PRXY,4,EMUc

TB,CONC,4,1,9,
TBDATA,,.2,.6,fgt,-1,,

Tb,czm,5,1,1,CBDD
Tbdata,1,480,.015,,,.01,

!Keypoints

K,1,
K,2,35.5
K,3,35.5,1.75
K,4,34.75,2.5
K,5,34.75,6
K,6,35.25,6.75
K,7,35.25,8.75
K,8,0,8.75
K,9,0,6.75
K,10,0,6
K,11,0,2.5
K,12,0,1.75
K,13,36,0
K,14,36,1.75
K,15,36,2.5
K,16,36,6
K,17,36,6.75
K,18,36,8.75
!Replicate Keypoints
KGEN,2,all,,,,,9
```

```
V,1,19,20,2,12,30,21,3
V,12,30,21,3,11,29,22,4
V,11,29,22,4,10,28,23,5
V,10,28,23,5,9,27,24,6
V,9,27,24,6,8,26,25,7

V,2,20,31,13,3,21,32,14
V,3,21,32,14,4,22,33,15
V,4,22,33,15,5,23,34,16
V,5,23,34,16,6,24,35,17
V,6,24,35,17,7,25,36,18

blc4,,,4,-1,9
blc4,22,8.75,4,1,9

!Move grout
vsel,s,,,6,10
vgen,2,all,,,10,,,,,,0
vdele,6,10
vsel,s,,,13,17
vgen,,all,,,-10,,,,,1

vsel,s,,,1,5
vsel,a,,,11,12
vglue,all
vsel,s,,,13,17
vglue,all

MSHAPE,0,3D     ! Use
hexahedra
Esize,1
!Mesh the Grout
Allsel,all
Vsel,s,,,13,17
Vatt,4,5,1
Vsweep,all
!mesh the Supports
Vsel,s,,,6,12,6
Vatt,2,1,2
Vsweep,all

!Mesh the Concr
Vsel,s,,,13,17
Vsel,a,,,6,12,6
Vsel,inve
```

```
Vatt,1,1,1
Vsweep,all

Allsel,all
Asel,s,,,4,24,5
Nsla,s,1
Type,4
Mat,5
Real,4
Tshape,quad
Esurf,,top

Allsel,all
Asel,s,,,61,81,5
Nsla,s,1
Type,5
Mat,1
Real,4
Esurf,,top

finish
/solu
!boundary conditions

asel,s,loc,x,36
nsla,s,1
d,all,ux
asel,s,loc,z
nsla,s,1
d,all,uz

asel,s,loc,y,-1
nsla,s,1
nsel,r,loc,x,2
d,all,uy

Asel,s,loc,x
Asel,u,,,86
sfa,all,1,pres,300

allsel,all
!—control parameters –
cnvtol,f,,0.05,2,.01
nsubst,25
outres,all,all
autots,1
!lnsrch,1
ncnv,2
neqit,50
pred,on
time,50
solve

asel,s,loc,y,9.75
nsla,s,1
nsel,r,loc,x,24
nsel,r,loc,z,9
f,all,fy,-350

asel,s,loc,y,9.75
nsla,s,1
nsel,r,loc,x,24
nsel,u,loc,z,9
f,all,fy,-700

allsel,all
!—control parameters –
cnvtol,f,,0.05,2,.01
nsubst,50
outres,all,all
autots,1
!lnsrch,1
ncnv,2
neqit,100
pred,on
time,100
solve

!24 Curved Bolt (Contact)

finish
/clear
/title, 24 inch Curved Bolt
/PREP7
!Steel area
area=0.44
! Concrete Elastic Modulus
Ec=3605000
Eg=4415201
! Concrete Poisson ratio
EMUc=0.2
! Concrete Compressive
and Tensile Strength
fc=4000
fg=6000
ft=480
fy=60000
fgt=575
sc=.002219
sg=.002718
! Elastic Modulus and
Poisson ratio for steel
Es=29e6
EMUs=0.3
! concrete element
ET,1,SOLID65
KEYOPT,1,3,2
KEYOPT,1,7,1
! steel element
ET,2,SOLID45
! rebar element
ET,3,LINK8
Et,4,targe170
Et,5,conta173
Keyopt,5,10,2
Keyopt,5,2,1
Keyopt,5,12,5
Keyopt,5,9,1
Keyopt,5,5,1

! Real constants
!R,1
R,1,3,0.009,0,90,3,.009,
RMORE,90,,!3,.009,,,
R,2,area
R,3,.7854,!1.037e-3
r,4
!R,5,,,.0036,,,,

MP,EX,1,Ec
MP,PRXY,1,EMUc

TB,CONC,1
TBDATA,,.2,.6,ft,-1,,
```

```
MP,EX,2,Es
MP,PRXY,2,EMUs
MP,EX,3,Es
MP,PRXY,3,EMUs
TB,BISO,3,,2
TBDAT,,fy,2900
Mp,alpx,3,12e-6

MP,EX,4,Eg
MP,PRXY,4,EMUc

TB,CONC,4,1,9,
TBDATA,,.2,.6,fgt,-1,,

Tb,czm,5,1,1,CBDD
Tbdata,1,480,.015,,,.01,

!Keypoints
K,1,
K,2,35.5
K,3,35.5,1.75
K,4,34.75,2.5
K,5,34.75,6
K,6,35.25,6.75
K,7,35.25,8.75
K,8,0,8.75
K,9,0,6.75
K,10,0,6
K,11,0,2.5
K,12,0,1.75
K,13,36,0
K,14,36,1.75
K,15,36,2.5
K,16,36,6
K,17,36,6.75
K,18,36,8.75
!Replicate Keypoints
KGEN,2,all,,,,,9

V,1,19,20,2,12,30,21,3
V,12,30,21,3,11,29,22,4
V,11,29,22,4,10,28,23,5
V,10,28,23,5,9,27,24,6
V,9,27,24,6,8,26,25,7
V,2,20,31,13,3,21,32,14
V,3,21,32,14,4,22,33,15
V,4,22,33,15,5,23,34,16
V,5,23,34,16,6,24,35,17
V,6,24,35,17,7,25,36,18

blc4,,,4,-1,9
blc4,10,8.75,4,1,9
wpoff,0,0,3
vsbw,all
wpoff,0,5
wprot,0,90
vsbw,all
wpoff,24.76433,-3,-1.75
wprot,0,0,56.065
vsel,s,,,21,22
vsbw,all
wprot,0,0,-90
vsel,s,,,9,11
vsbw,all
wpstyl,defa
wpoff,37.71582
wprot,-31.95315,90
vsel,s,,,10,12,2
vsel,a,,,17,18
vsbw,all
wprot,0,0,31.95315
wpoff,2.6181
wprot,0,0,-26.66721
vsel,s,,,19,20
vsbw,all
wprot,0,0,26.66721
wpoff,5.00811
wprot,0,0,-19.48794
vsel,s,,,3,4
vsbw,all
wprot,0,0,19.48794
wpoff,14.16683
wprot,0,0,-10.02097
vsel,s,,,1,2
vsbw,all
wprot,0,0,10.02097
wpoff,0,0,-4.375
vsel,s,,,5,6
vsbw,all
wprot,0,-90
wpoff,0,0,1.5
vsel,all
vsbw,all
wpstyl
btol,2.5632923e-4

!Move grout
vsel,s,,,1,7,6
vsel,a,,,23,25,2
vsel,a,,,29,31,2
vsel,a,,,45,51,6
vsel,a,,,54,59
vsel,a,,,67,68
vsel,a,,,70,71
vsel,a,,,80,82
vgen,2,all,,,10,,,,,,0
vsel,s,,,1,7,6
vsel,a,,,23,25,2
vsel,a,,,29,31,2
vsel,a,,,45,51,6
vsel,a,,,54,59
vsel,a,,,67,68
vsel,a,,,70,71
vsel,a,,,80,82
vdele,all,,,1
vsel,s,,,2,11,9
vsel,a,,,4,16,4
vsel,a,,,14,30,4
vsel,a,,,24,27,3
vsel,a,,,32,33
vsel,a,,,35,38,3
vsel,a,,,40,42
vsel,a,,,44
vgen,,all,,,-10,,,,,1

vsel,s,,,2,11,9
vsel,a,,,4,16,4
vsel,a,,,14,30,4
vsel,a,,,24,27,3
vsel,a,,,32,33
vsel,a,,,35,38,3
vsel,a,,,40,42
vsel,a,,,44
vsel,inve
```

```
vglue,all
vsel,s,,,2,11,9
vsel,a,,,4,16,4
vsel,a,,,14,30,4
vsel,a,,,24,27,3
vsel,a,,,32,33
vsel,a,,,35,38,3
vsel,a,,,40,42
vsel,a,,,44
vglue,all

lsel,s,,,95
lsel,a,,,262,272,10
lsel,a,,,333,355,22
lsel,a,,,410
lglue,all

!--resize lines for meshing
Lsel,s,length,,6
Lsel,a,length,,1.5
Lesize,all,.75

Lsel,s,length,,9,34
Lsel,a,length,,4
!Lsel,a,,,176
Lesize,all,1

Allsel,all
Esize,1

!--Mesh Grout
vsel,s,,,2,11,9
vsel,a,,,4,16,4
vsel,a,,,14,30,4
vsel,a,,,24,27,3
vsel,a,,,32,33
vsel,a,,,35,38,3
vsel,a,,,40,42
vsel,a,,,44
Vatt,4,4,1
Vsweep,all
!--Mesh the Curved Bolt
lsel,s,,,95
lsel,a,,,262,272,10
lsel,a,,,333,355,22
lsel,a,,,2
latt,3,3,3
Lmesh,all
!--Mesh the Supports
Vsel,s,,,1,7,6
Vsel,a,,,23,36,13
Vsel,a,,,63,73,10
Vsel,a,,,49,50
Vsel,a,,,75,76
Vatt,2,1,2
Vsweep,all

!--Mesh Concret
vsel,s,,,2,11,9
vsel,a,,,4,16,4
vsel,a,,,14,30,4
vsel,a,,,24,27,3
vsel,a,,,32,33
vsel,a,,,35,38,3
vsel,a,,,40,42
vsel,a,,,44
Vsel,a,,,1,7,6
Vsel,a,,,23,36,13
Vsel,a,,,63,73,10
Vsel,a,,,49,50
Vsel,a,,,75,76
Vsel,inve
Vatt,1,1,1
Vsweep,all

Allsel,all
Asel,s,,,16,19,3
Asel,a,,,29,63,34
Asel,a,,,71,85,14
Asel,a,,,92,176,84
Asel,a,,,188,210,22
Asel,a,,,214,224,10
Asel,a,,,229,237,4
Asel,a,,,246,261,15
Asel,a,,,264,282,18
Asel,a,,,307,310,3
Nsla,s,1
Type,4
Mat,5
Real,5
Tshape,quad
Esurf,,top

Allsel,all
Asel,s,,,24,67,43
Asel,a,,,78,94,16
Asel,a,,,107,122,15
Asel,a,,,124,133,9
Asel,a,,,146,161,15
Asel,a,,,175,322,147
Asel,a,,,326,331,5
Asel,a,,,337,349,3
Asel,a,,,353,355,2
Nsla,s,1
Type,5
Mat,1
Real,5
Esurf,,top

finish
/solu
!boundary conditions
allsel,all
asel,s,loc,x,36
nsla,s,1
d,all,ux
asel,s,loc,z
nsla,s,1
d,all,uz

asel,s,loc,y,-1
nsla,s,1
nsel,r,loc,x,2
d,all,uy

lsel,s,,,95
lsel,a,,,262,272,10
lsel,a,,,333,355,22
lsel,a,,,2
bfl,all,temp,-115

allsel,all
!—control parameters –
cnvtol,f,,0.05,2,.01
nsubst,25
```

```
outres,all,all
autots,1
!lnsrch,1
ncnv,2
neqit,50
pred,on
time,50
solve

asel,s,loc,y,9.75
nsla,s,1
nsel,r,loc,x,12
nsel,r,loc,z,9
f,all,fy,-325!crack180
ult325

asel,s,loc,y,9.75
nsla,s,1
nsel,r,loc,x,12
nsel,u,loc,z,9
f,all,fy,-650 !crack360
ult650

allsel,all
!—control parameters –
cnvtol,f,,0.05,2,.01
nsubst,200
outres,all,all
autots,1
!lnsrch,1
ncnv,2
neqit,250
pred,on
time,300
solve

!36 Curved Bolt (Contact)

finish
/clear
/title, 36 inch Curved Bolt
/PREP7
!Steel area
area=0.44
```

```
! Concrete Elastic Modulus
Ec=3605000
Eg=4415201
! Concrete Poisson ratio
EMUc=0.2
! Concrete Compressive
and Tensile Strength
fc=4000
fg=6000
ft=480
fy=60000
fgt=575
sc=.002219
sg=.002718
! E and PR for steel
Es=29e6
EMUs=0.3
! concrete element
ET,1,SOLID65
KEYOPT,1,3,2
KEYOPT,1,7,1
! steel element
ET,2,SOLID45
! rebar element
ET,3,LINK8
Et,4,targe170
Et,5,conta173
Keyopt,5,10,2
Keyopt,5,2,1
Keyopt,5,12,5
Keyopt,5,9,1
Keyopt,5,5,1
! Real constants
!R,1
R,1,3,0.009,0,90,3,.009,
RMORE,90,,!3,.009,,,
R,2,area
R,3,.60132,!1.354e-3
r,4,
!R,5,,,.0036,,,,

MP,EX,1,Ec
MP,PRXY,1,EMUc
mptemp,1,0
```

```
TB,CONC,1
TBDATA,,.2,.6,ft,-1,,

MP,EX,2,Es
MP,PRXY,2,EMUs
MP,EX,3,Es
MP,PRXY,3,EMUs
TB,BISO,3,,2
TBDAT,,fy,2900
Mp,alpx,3,12e-6
MP,EX,4,Eg
MP,PRXY,4,EMUc

TB,CONC,4,1,9,
TBDATA,,.2,.6,fgt,-1,,

Tb,czm,5,1,1,CBDD
Tbdata,1,480,.015,,,.01,

!Keypoints

K,1,
K,2,35.5
K,3,35.5,1.75
K,4,34.75,2.5
K,5,34.75,6
K,6,35.25,6.75
K,7,35.25,8.75
K,8,0,8.75
K,9,0,6.75
K,10,0,6
K,11,0,2.5
K,12,0,1.75
K,13,36,0
K,14,36,1.75
K,15,36,2.5
K,16,36,6
K,17,36,6.75
K,18,36,8.75
!Replicate Keypoints
KGEN,2,all,,,,,9

V,1,19,20,2,12,30,21,3
V,12,30,21,3,11,29,22,4
V,11,29,22,4,10,28,23,5
```

```
V,10,28,23,5,9,27,24,6
V,9,27,24,6,8,26,25,7

V,2,20,31,13,3,21,32,14
V,3,21,32,14,4,22,33,15
V,4,22,33,15,5,23,34,16
V,5,23,34,16,6,24,35,17
V,6,24,35,17,7,25,36,18

blc4,,,4,-1,9
blc4,22,8.75,4,1,9
wpoff,0,0,3
vsbw,all
wpoff,0,5
wprot,0,90
vsbw,all
wpoff,19.871,-3,-1.75
wprot,0,0,66.232
vsel,s,,,21,22
vsbw,all
wprot,0,0,-90
vsel,s,,,9,11
vsbw,all
wpstyl,defa
wpoff,39.40066
wprot,-21.8416,90
vsel,s,,,10,12,2
vsel,a,,,17,18
vsbw,all
wprot,0,0,21.8416
wpoff,3.57277
wprot,0,0,-18.29716
vsel,s,,,19,20
vsbw,all
wprot,0,0,18.29716
wpoff,7.04523
wprot,0,0,-13.39733
vsel,s,,,3,4
vsbw,all
wprot,0,0,13.39733
wpoff,24.79572
wprot,0,0,-6.23196
vsel,s,,,1,2
vsbw,all
wprot,0,0,6.23196
wpoff,0,0,-4.375
vsel,s,,,5,6
vsbw,all
wprot,0,-90
wpoff,0,0,1.5
vsel,all
vsbw,all
wpstyl
btol,5e-4

!Move grout
vsel,s,,,1,7,6
vsel,a,,,23,25,2
vsel,a,,,29,31,2
vsel,a,,,45,51,6
vsel,a,,,54,59
vsel,a,,,67,68
vsel,a,,,70,71
vsel,a,,,80,82
vgen,2,all,,,10,,,,,,0
vsel,s,,,1,7,6
vsel,a,,,23,25,2
vsel,a,,,29,31,2
vsel,a,,,45,51,6
vsel,a,,,54,59
vsel,a,,,67,68
vsel,a,,,70,71
vsel,a,,,80,82
vdele,all,,,1
vsel,s,,,2,11,9
vsel,a,,,4,16,4
vsel,a,,,14,30,4
vsel,a,,,24,27,3
vsel,a,,,32,33
vsel,a,,,35,38,3
vsel,a,,,40,42
vsel,a,,,44
vgen,,all,,,-10,,,,,1

vsel,s,,,2,11,9
vsel,a,,,4,16,4
vsel,a,,,14,30,4
vsel,a,,,24,27,3
vsel,a,,,32,33
vsel,a,,,35,38,3
vsel,a,,,40,42
vsel,a,,,44
vsel,inve
vglue,all
vsel,s,,,2,11,9
vsel,a,,,4,16,4
vsel,a,,,14,30,4
vsel,a,,,24,27,3
vsel,a,,,32,33
vsel,a,,,35,38,3
vsel,a,,,40,42
vsel,a,,,44
vglue,all

lsel,s,,,95
lsel,a,,,262,272,10
lsel,a,,,333,355,22
lsel,a,,,410
lglue,all

!--resize lines for meshing
Lsel,s,length,,6
Lsel,a,length,,1.5
Lesize,all,.75

Lsel,s,length,,6.5,36
Lsel,a,length,,4
Lesize,all,1
Lsel,s,length,,.25,1.25
Lesize,all,,2

Allsel,all
Esize,1

!--Mesh Grout
vsel,s,,,2,11,9
vsel,a,,,4,16,4
vsel,a,,,14,30,4
vsel,a,,,24,27,3
vsel,a,,,32,33
vsel,a,,,35,38,3
vsel,a,,,40,42
vsel,a,,,44
Vatt,4,4,1
Vsweep,all
```

```
!--Mesh the Curved Bolt
lsel,s,,,95
lsel,a,,,262,272,10
lsel,a,,,333,355,22
lsel,a,,,2
!lsel,a,,,410
latt,3,3,3
Lmesh,all
!--Mesh the Supports
Vsel,s,,,1,7,6
Vsel,a,,,23,36,13
Vsel,a,,,63,73,10
Vsel,a,,,49,50
Vsel,a,,,75,76
Vatt,2,1,2
Vsweep,all

!--Mesh Concret
vsel,s,,,2,11,9
vsel,a,,,4,16,4
vsel,a,,,14,30,4
vsel,a,,,24,27,3
vsel,a,,,32,33
vsel,a,,,35,38,3
vsel,a,,,40,42
vsel,a,,,44
Vsel,a,,,1,7,6
Vsel,a,,,23,36,13
Vsel,a,,,63,73,10
Vsel,a,,,49,50
Vsel,a,,,75,76
Vsel,inve
Vatt,1,1,1
Vsweep,all

Allsel,all
Asel,s,,,16,19,3
Asel,a,,,29,63,34
Asel,a,,,71,85,14
Asel,a,,,92,176,84
Asel,a,,,188,210,22
Asel,a,,,214,224,10
Asel,a,,,229,237,4
Asel,a,,,246,261,15
Asel,a,,,264,282,18
Asel,a,,,307,310,3
Nsla,s,1
Type,4
Mat,5
Real,5
Tshape,quad
Esurf,,top

Allsel,all
Asel,s,,,24,67,43
Asel,a,,,78,94,16
Asel,a,,,107,122,15
Asel,a,,,124,133,9
Asel,a,,,146,161,15
Asel,a,,,175,322,147
Asel,a,,,326,331,5
Asel,a,,,337,349,3
Asel,a,,,353,355,2
Nsla,s,1
Type,5
Mat,1
Real,5
Esurf,,top

finish
/solu
!boundary conditions
allsel,all
asel,s,loc,x,36
nsla,s,1
d,all,ux
asel,s,loc,z
nsla,s,1
d,all,uz

asel,s,loc,y,-1
nsla,s,1
nsel,r,loc,x,2
d,all,uy

!Asel,s,loc,x
!Asel,u,,,30,34,4
!Asel,u,,,4
!sfa,all,1,pres,300

lsel,s,,,95
lsel,a,,,262,272,10
lsel,a,,,333,355,22
lsel,a,,,2
bfl,all,temp,-130

allsel,all
!—control parameters –
cnvtol,f,,0.05,2,.01
nsubst,25
outres,all,all
autots,1
ncnv,2
neqit,50
pred,on
time,50
solve

asel,s,loc,y,9.75
nsla,s,1
nsel,r,loc,x,24
nsel,r,loc,z,9
f,all,fy,-225 !Crack104.5
ult225

asel,s,loc,y,9.75
nsla,s,1
nsel,r,loc,x,24
nsel,u,loc,z,9
f,all,fy,-450 !Crack209
ult450

allsel,all
!—control parameters –
cnvtol,f,,0.05,2,.01
nsubst,100
outres,all,all
autots,1
ncnv,2
neqit,100
pred,on
time,200
solve
```

!Welded Stud (Contact)

```
finish
/clear
/title, Welded Stud
/PREP7
!Steel area
area=0.2
! Concrete Elastic Modulus
Ec=3605000
Eg=4415201
! Concrete Poisson ratio
EMUc=0.2
! Concrete Compressive
and Tensile Strength
fc=4000
fg=6000
ft=480
fy=60000
fgt=575
! Elastic Modulus and
Poisson ratio for steel
Es=29e6
EMUs=0.3
! concrete element
ET,1,SOLID65
KEYOPT,1,3,2
KEYOPT,1,7,1
! steel element
ET,2,SOLID45
! rebar element
ET,3,LINK8
! Real constants
Et,4,targe170
Et,5,conta173
Keyopt,5,10,2
Keyopt,5,2,1
Keyopt,5,12,5
Keyopt,5,9,1
Keyopt,5,5,1

R,1
R,1,3,0.009,0,90,3,.009,
RMORE,90, , , , , ,
R,2,area
R,3,1.227
R,4,
R,5,,,.0036,,,,

MP,EX,1,Ec
MP,PRXY,1,EMUc

TB,CONC,1
TBDATA,,.2,.6,ft,-1,,

MP,EX,2,Es
MP,PRXY,2,EMUs
MP,EX,3,Es
MP,PRXY,3,EMUs
TB,BISO,3,,2
TBDAT,,fy,2900

MP,EX,4,Eg
MP,PRXY,4,EMUc

TB,CONC,4,1,9,
TBDATA,,.2,.6,fgt,-1,,

Tb,czm,5,1,1,CBDD
Tbdata,1,480,.016,,,.01,

!add all keypoints
K,1,
K,2,35.8125
K,3,35.8125,3.75
K,4,33.5,5.75
K,5,35,7.75
K,6,35,8.75
K,7,33.5,8.75
K,8,0,8.75
K,9,0,7.75
K,10,0,5.75
K,11,0,3.75
K,12,33.5,7.75
K,13,36
K,14,36,3.75
K,15,36,5.75
K,16,36,7.75
K,17,36,8.75

!Replicate Keypoints
KGEN,2,all,,,,,3
KGEN,2,1,17,,,,9

!Create volumes through
keypoints
V,1,18,19,2,11,28,20,3
V,11,28,20,3,10,27,21,4
V,10,27,21,4,9,26,29,12
V,9,26,29,12,8,25,24,7
V,4,21,22,5,7,24,23,6

V,3,20,31,14,4,21,32,15
V,4,21,32,15,5,22,33,16
V,5,22,33,16,6,23,34,17

V,18,35,36,19,28,45,37,20
V,28,45,37,20,27,44,38,21
V,27,44,38,21,26,43,46,29
V,26,43,46,29,25,42,41,24
V,21,38,39,22,24,41,40,23

V,20,37,48,31,21,38,49,32
V,21,38,49,32,22,39,50,33
V,22,39,50,33,23,40,51,34
blc4,,,4,-1,9
blc4,22,8.75,4,1,9
wpoff,0,0,1.5
vsbw,all
wpoff,33.5,3.75
wprot,40.85537626,90
vsel,s,,,19,22
vsel,a,,,9,10
vsbw,all
wprot,0,-90
wprot,-40.85537626
wpoff,0,4
wprot,0,90
allsel,all
vsbw,all
wpoff,0,0,6.75
vsbw,all
wpstyl
allsel,all

!Move grout
```

```
vsel,s,,,29,34
vsel,a,,,14,16
vsel,a,,,10,19,9
vsel,a,,,21,22
vgen,2,all,,,10,,,,,,0
vsel,s,,,29,34
vsel,a,,,14,16
vsel,a,,,10,19,9
vsel,a,,,21,22
vdele,all,,,1
vsel,s,,,4,8
vsel,a,,,17
vsel,a,,,50,56
vgen,,all,,,-10,,,,,1

vsel,s,,,4,8
vsel,a,,,17
vsel,a,,,50,56
vsel,inve
vglue,all

vsel,s,,,4,8
vsel,a,,,17
vsel,a,,,50,56
vglue,all

!Glue stud and plate
Lsel,s,,,68
Lsel,a,,,266,272,3
Lsel,a,,,297
Lsel,a,,,311,313
Lsel,a,,,317,325
Lsel,a,,,38
Lsel,a,,,234
Lglue,all

Lsel,s,length,,6
Lsel,a,length,,1.5
Lesize,all,.75
Lsel,s,length,,4
Lsel,a,length,,7,36
Lesize,all,1

Allsel,all
Esize,1

Mshkey,1
MSHAPE,0,3D

!Mesh Grout
vsel,s,,,4,8
vsel,a,,,17
vsel,a,,,50,56
Vatt,4,4,1
Vsweep,all

!Mesh Plate
Lsel,s,,,24,25
Lsel,a,,,32,33
Lsel,a,,,68
Lsel,a,,,266,272,3
Lsel,a,,,297
Lsel,a,,,313,317,4
Lsel,a,,,319,323
Lsel,a,,,325
Latt,3,3,3
Lmesh,all

!Mesh Concrete
vsel,s,,,1,8
vsel,a,,,15,17
vsel,a,,,50,56
Vsel,a,,,35,37,2
Vsel,a,,,27,28
Vsel,a,,,13
Vsel,a,,,43,49,3
Vsel,inve
Vatt,1,1,1
Vsweep,all

!Concrete without Rebar
Vsel,s,,,1,3
Vsel,a,,,13
Vsel,a,,,27,28
Vsel,a,,,43,49,3
Vatt,1,4,1
Vsweep,all

!Mesh Stud
Lsel,s,,,38
Lsel,a,,,234
Latt,3,2,3
Lmesh,all

!Mesh Supports
Vsel,s,,,35,37,2
Vsel,a,,,15,16
Vatt,2,,2
Vsweep,all

Allsel,all
Asel,s,,,25,32,7
Asel,a,,,42,44,2
Asel,a,,,200,207,7
Asel,a,,,84
Asel,a,,,212,214
Asel,a,,,221,222
Asel,a,,,225,226
Nsla,s,1
Type,4
Mat,5
Real,5
Tshape,quad
Esurf,,top

Allsel,all
Asel,s,,,3,6,3
Asel,a,,,12,19,7
Asel,a,,,35,58,23
Asel,a,,,61,87,26
Asel,a,,,106,113,7
Asel,a,,,123,160,37
Asel,a,,,163,165,2
Nsla,s,1
Type,5
Mat,1
Real,5
Esurf,,top

finish
/solu
!boundary conditions
allsel,all
asel,s,loc,x,36
nsla,s,1
```

```
d,all,ux
asel,s,loc,z
nsla,s,1
d,all,uz

asel,s,loc,y,-1
nsla,s,1
nsel,r,loc,x,2
d,all,uy

asel,s,loc,y,9.75
nsla,s,1
nsel,r,loc,x,24
nsel,r,loc,z,9
f,all,fy,-100

asel,s,loc,y,9.75
nsla,s,1
nsel,r,loc,x,24
nsel,u,loc,z,9
f,all,fy,-200

allsel,all
!—control parameters –
cnvtol,f,,0.05,2,.01
nsubst,100
outres,all,all
autots,1
!lnsrch,1
ncnv,2
neqit,200
pred,on
time,50
solve
```